DNA and Chromosomes:

Dna2 Is Involved in CA Strand Resection and Nascent Lagging Strand Completion at Native Yeast Telomeres

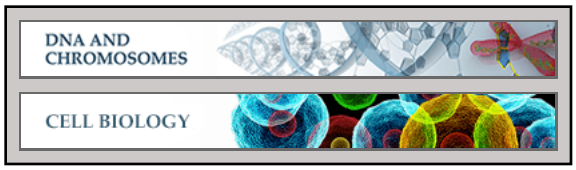

Martin E. Budd and Judith L. Campbell

J. Biol. Chem. 2013, 288:29414-29429.
doi: 10.1074/jbc.M113.472456 originally published online August 20, 2013

THE JOURNAL OF BIOLOGICAL CHEMISTRY VOL. 288, NO. 41, pp. 29414–29429, October 11, 2013

Dna2 Is Involved in CA Strand Resection and Nascent Lagging Strand Completion at Native Yeast Telomeres*

Received for publication, March 26, 2013, and in revised form, August 19, 2013 Published, JBC Papers in Press, August 20, 2013, DOI 10.1074/jbc.M113.472456

Martin E. Budd and Judith L. Campbell[1]

From Braun Laboratories, California Institute of Technology, Pasadena, California 91125

Background: DNA2 helicase/nuclease participates in telomere maintenance by unknown mechanisms.
Results: *dna2* mutants show slightly shortened telomeric GT-overhangs and accumulate small, nascent lagging strand DNA chains at telomeres.
Conclusion: Unlike at DSBs, additional nucleases largely compensate for the simultaneous loss of Dna2 and Mre11 in producing GT.
Significance: FEN1, Dna2, or Exo1 is necessary to mature lagging strands at telomeres.

Post-replicational telomere end processing involves both extension by telomerase and resection to produce 3′-GT-overhangs that extend beyond the complementary 5′-CA-rich strand. Resection must be carefully controlled to maintain telomere length. At short *de novo* telomeres generated artificially by HO endonuclease in the G_2 phase, we show that *dna2*-defective strains are impaired in both telomere elongation and sequential 5′-CA resection. At native telomeres in *dna2* mutants, GT-overhangs do clearly elongate during late S phase but are shorter than in wild type, suggesting a role for Dna2 in 5′-CA resection but also indicating significant redundancy with other nucleases. Surprisingly, elimination of Mre11 nuclease or Exo1, which are complementary to Dna2 in resection of internal double strand breaks, does not lead to further shortening of GT-overhangs in *dna2* mutants. A second step in end processing involves filling in of the CA-strand to maintain appropriate telomere length. We show that Dna2 is required for normal telomeric CA-strand fill-in. Yeast *dna2* mutants, like mutants in DNA ligase 1 (*cdc9*), accumulate low molecular weight, nascent lagging strand DNA replication intermediates at telomeres. Based on this and other results, we propose that FEN1 is not sufficient and that either Dna2 or Exo1 is required to supplement FEN1 in maturing lagging strands at telomeres. Telomeres may be among the subset of genomic locations where Dna2 helicase/nuclease is essential for the two-nuclease pathway of primer processing on lagging strands.

Yeast telomeres end in ~300 bp of short repeated sequences that are GT-rich in the 3′-terminating strand and CA-rich in the 5′-terminating strand (1, 2). Yeast telomeres replicate in late S/G_2 from late-firing subtelomeric origins of replication (autonomously replicating sequence). Because the replication fork most frequently proceeds outward toward the end of the chromosome, the nascent telomere GT-strand is synthesized by the leading strand polymerase, and the CA-strand is synthesized by the lagging strand polymerase. In yeast, as in many organisms, the telomeres are not fully duplex but have single-stranded GT-overhangs. Yeast GT-overhangs are about 12–14 nucleotides long in G_1 and double in length during S phase (3, 4). Overhangs occur on both leading and lagging strands (5–7), but it is not known if they are generated in the same way on both ends. Synthesis of the CA-strand by the lagging strand polymerase is predicted to leave a short unreplicated segment. This could either be due to RNA primer removal or to the uncoupling of the leading and lagging strands, *i.e.* absence of the replisome (8), resulting in a single-stranded 3′-GT-overhang. Nucleolytic resection of the CA-strand might also contribute to the lagging strand 5′-GT-overhang. The end replicated by the leading strand assembly, however, is expected to have a blunt end and would require 5′- to 3′-nucleolytic resection to create a 3′-GT-overhang, suggesting that the overhangs arise due to resection (9). A number of helicases and nucleases are known to participate in these processes, but the precise pathways are still unclear.

The GT-overhangs are extended by telomerase, which, in effect, prevents erosion of the chromosome end (10). How the number of repeats added by telomerase is regulated and how the complementary lagging strand is synthesized and matured, referred to as CA-strand fill-in, are not completely understood. Also poorly understood is how aberrant recombination and checkpoint activation is prevented. Understanding regulation of telomerase and the DNA damage checkpoint, respectively, requires understanding the roles of numerous proteins, including Mre11, Rad50, Tel1, Xrs2, Dna2, Est1, Est3, Cdc13, Stn1, Ten1, Pif1, Rap1, Rif1, Rif2, RPA, Ku70/Ku80, and the entire lagging strand replication machinery (11–22).

Dna2 is a 5′- to 3′-helicase specific for forked substrates and a 5′- to 3′-and 3′- to 5′-exo/endonuclease (23–27). Dna2 and FEN1 are assumed to work together in the "two-nuclease" pathway of RNA primer removal during Okazaki fragment processing (22, 28–41). A third nuclease, Exo1, can substitute for FEN1 or Dna2 in some instances. It is not clear where in the genome the two-nuclease pathway is required. However, telomeres are one possibility, because replication forks are known to stall within the duplex GT-rich repeats, indicating they pose difficulties for the processive replisome and because bulk Dna2 localizes to telomeres from yeast to mammals (42–44).

* This work was supported, in whole or in part, by National Institutes of Health Grant GM078666. This work was also supported by Ellison Foundation Grant AG-SS-2143-08.
[1] To whom correspondence should be addressed: Braun Laboratories, Caltech, 1200 E. California Blvd., MC 147-75, Pasadena, CA 91125. Tel.: 626-395-6053; E-mail: jcampbel@caltech.edu.

Dna2 has a second critical function, namely in homology-directed recombination. In conjunction with the Sgs1 RecQ helicase, Dna2 catalyzes long range resection of the 5′ strand at intra-chromosomal DSBs[2] to initiate homology-directed recombination and checkpoint activation (45–47). Exo1 acts redundantly with Dna2 in long range resection. Interestingly, Mre11 nuclease also functions in resection and becomes essential for DSB repair in the absence of Dna2 and vice versa (46, 48). FEN1 has also recently been detected by ChIP assays at an HO-induced DSB (in *Schizosaccharomyces pombe*) (49), and overexpression of FEN1 suppresses the x-ray sensitivity of *dna2-1* mutants (50). It is striking that the same nucleases used in Okazaki fragment processing also function in DSB resection.

Dna2 associates in bulk with telomeres during G_1, dissociates from telomeres during S phase, moving to many other chromosomal sites, and then reassociates with telomeres at late S/G_2 phase. Just as in S phase, Dna2 is also displaced from telomeres when cells undergo bleomycin-induced DSB DNA damage (42). This release may facilitate the recruitment of Dna2 for resection and activation of the Mec1 checkpoint kinase (51, 52). We have previously shown that *dna2-2* mutants are defective in telomerase-dependent telomere lengthening and that *dna2-2 est1*Δ and *dna2-2 est2*Δ mutants senesce dramatically more rapidly than *est1*Δ (subunit of telomerase) or *est2*Δ (telomerase) single mutants (42, 53). In the double mutants, survivors arise more rapidly than in single telomerase mutants, and double-mutant survivors occur almost exclusively due to break-induced replication in the GT/CA tracts, rather than by Y′-dependent recombination (42). Biochemically, we demonstrated that Dna2 binds DNA-containing telomeric GT-rich repeats that form G quadruplexes (G4) and G4 secondary structures much more avidly than single-stranded DNA. Both yeast and human Dna2 unwind G4 structures and cleave the DNA at junctions between single-stranded DNA G4 structures (43, 54). Thus, another function of Dna2 may be to resolve G4 structures that impede replication at telomeres.

Exo1 and Mre11 also play roles at telomeres. Exo1 creates long regions of single-stranded DNA at uncapped telomeres in *cdc13* mutants and is involved in resection of a *de novo* telomere in G_2-arrested cells (see Fig. 1). In this artificial telomere resection assay, Exo1 is redundant with Dna2 (55–59). Overhang production at native, equilibrating telomeres in late S phase has not been studied in *exo1* or *dna2* mutants, however. Mre11 also functions in multiple capacities at telomeres, deletion mutants evidencing short telomeres, and short GT-overhangs (5, 12, 60).

Here, we show that S phase GT-overhangs are shorter in *dna2* mutants but not completely absent, confirming a role in telomere resection at native, equilibrating telomeres as well as at short *de novo* telomeres. Unlike at DSBs (45, 46, 48, 61), however, we were surprised to find that inactivation of Mre11 or Exo1 did not further reduce overhangs at native telomeres. This could be due to a delay in CA-strand fill-in, because we demonstrate that nascent lagging strands accumulate as fragments shorter than 3 kb in *dna2* mutants, consistent with its role in flap removal during Okazaki fragment processing, just as in DNA ligase or FEN1 mutants. Thus, Dna2 has at least two roles at native telomeres.

[2] The abbreviations used are: DSB, double strand break; G4, G quadruplex; Ch, chromosomal region; RI, replication intermediate; pol, polymerase; nt, nucleotide.

EXPERIMENTAL PROCEDURES

Strains Used—The strains are listed in Table 1.

De Novo Telomere Addition—The *de novo* telomere addition and resection assays were carried out as described previously (13, 21, 42). Strains UCC5913 and UCC5913 *dna2-1* were grown in SC-lysine media overnight, collected by centrifugation, resuspended in YP-2.5% raffinose media, and grown to a cell density of 10^7 cells/ml at 23 °C. Nocodazole (10 μg/ml) was added and incubation continued until 95% of the cells appeared as dumbbells. Cells were collected by centrifugation, resuspended in YP-3% galactose, and incubated at the appropriate temperature. Chromosomal DNA was isolated on Qiagen P20 columns. For telomere addition assays, the DNA was digested with SpeI, electrophoresed on a 1% agarose gel, blotted by capillary transfer onto GeneScreen Plus with 0.1 M NaOH, and hybridized with the *ADE2* proximal probe. The *ADE2* probe was synthesized as a PCR product created with oligonucleotides ADE2–5′ and ADE2–3′. The distal probe was synthesized as a PCR product with oligonucleotides ADH-HO and NotI-ADH.

De Novo Telomere Resection—For resection assays, DNA was digested with DdeI, electrophoresed on a 5% denaturing polyacrylamide gel, and transferred with a Trans-Blot semi-dry electrophoretic transfer cell (Bio-Rad). The CA-terminating strand on the blot was hybridized with an *ADE2* strand-specific riboprobe synthesized from a PCR product created with oligonucleotides ADE2-RIBO-5′-CA and ADE2-RIBO-3′-CA. Data were quantified using the PhosphorImager and ImageQuant software. The fraction remaining was obtained by scanning the 287-bp control band and the 300-bp terminal band with the PhosphorImager and dividing the counts from the 300-bp band by those in the 287-bp band.

Native Telomere Analysis—Native telomere single-stranded 3′-GT tails were analyzed by growing *bar1*Δ cells to 10^7 cells/ml and adding α factor to a concentration of 50 ng/ml. WT and *pif1*Δ cells arrested with 95% G_1 cells. *dna2*Δ *pif1*Δ and *mre11-H125N pif1*Δ cells arrested with 90% G_1 cells. *dna2*Δ *pif1*Δ *mre11D56N, dna2*Δ *pif1*Δ *mre11H56N,* and *mre11*Δ *pif1*Δ cells arrested with 80% G_1 cells. Cells arrested in α factor were collected by centrifugation, washed with water, and resuspended in YPD media at 30 °C containing 0.1 mg/ml Pronase. Cells were incubated at the indicated temperatures and harvested at various time points. Chromosomal DNA was isolated with Qiagen P100 columns and digested with XhoI. DNA was quantified by gel electrophoresis and UV absorption. Equal amounts of DNA were electrophoresed on 0.7% agarose gels, blotted onto GeneScreen Plus by capillary transfer with 1× SSC, *i.e.* without denaturation, and hybridized with the telomere-specific oligonucleotide probe ACCCACCACACACCCACCCA at 37 °C in 5× SSC, 5× Denhardt's, 0.01 $Na_4P_2O_7$, 0.01 Na_2PO_4, 0.5% SDS and washed with 0.2% SSC, 0.2% SDS at 33 °C (62). The same DNAs, 0.1 volume, were also blotted with 0.1 M NaOH and hybridized with 6×10^4 cpm/ml of the CA probe or with 3 ×

TABLE 1

Strains and oligonucleotides

ADH4-HO and NOT1-ADH probes are described in Diede and Gottschling (21).

	Strains
BY4741	*MATa his3Δ1 leu2Δ0 met15Δ0 ura3Δ0* (Open Biosytems)
BY1408	4741 *MATa bar1Δ::KANMX* (Open Biosystems)
MB120-5A	4742 *MATα bar1Δ:: KANMX trp1Δ* (51)
MB121	4741 *MATa pif1Δ::HIS3 bar1Δ:: KANMX* (46)
MB122-17C	4741 *MATa mre11Δ::NATR bar1Δ::KANMX trp1D* (46)
MB124-2D	4741 *MATa mre11Δ::NATR pif1Δ::HIS3 bar1Δ::KANMX trp1Δ* (46)
MB128	4741 *MATa mre11Δ::NATR mre11-D56N::URA3 pif1Δ::HIS3 bar1Δ::kanMX* (46)
MB129	4741 *MATa mre11Δ::NATRmre11-H125N::URA3 pif1Δ::HIS3 bar1Δ::kanMX* (46)
MB161B	4741 *MATa dna2Δ::KANMX* pif1Δ::*HIS3 trp1Δ bar1Δ::KANMX* (46)
MB161B-56	4741 *MATa dna2Δ::kanMX pif1Δ::HIS3 mre11Δ::natR mre11-D56N::URA3 trp1Δ bar1Δ::kanMX* (46)
MB161B-125	4741 *MATa dna2Δ::kanMX pif1Δ::HIS3 mre11Δ::natRmre11-H125N::URA3 trp1Δ bar1Δ::kanMX* (46)
MB214	*MATa dna2-2::LEU2 ura3 leu2 his3* (this work)
MB215	*MATa cdc13-1 ura3 leu2 his3 lys2-801* (this work)
MB216	*MATa exo1Δ:: kanMX ura3 leu2 his2 lys2-801* (this work)
MB217	*MATa dna2-2::LEU2 exo1Δ::kanMX ura3 leu2 his3* (this work)
UCC5913	*MATa-inc ura3-52 lys2-801 ade2-101 trp1-Δ63 his3-Δ200 leu2-Δ1:LEU2-ALHO VII-L::ADE2-TG-HOsite-LYS2* (21)
UCC5913-2-1	UCC5913 *dna2-1* (this work)
NK-26	*MATa ura3-52 trp1-289 leu2-3,112 bar1::LEU2 cdc9-1 rad9⊗::URA3*
MB220	*MATa dna2-1 his3⊗1 leu2⊗0 met15⊗0 ura3⊗0 trp1⊗ bar1⊗::NatR*
MB221	*MATa dna2-1 rad9⊗::kanMX his3⊗1 leu2⊗0 met15⊗0 ura3⊗0 trp1⊗ bar1⊗::NatR*
MB222	*MATa dna2⊗ rad9-320 his3⊗1 leu2⊗0 met15⊗0 ura3⊗0 trp1⊗ bar1⊗::NatR*
MB223	*MATa cdc9-1 his3⊗1 leu2⊗0 met15⊗0 ura3⊗0 bar1⊗::NatR*
Oligonucleotides used as primers for various probes	
CA	5′ ACCCACCACACACACCCACACCCA
GT	5′ GTGGGTGTGGGTGTGTGTGGT
Y′/GT boundary	5′ CTCTCTCACATCTACCTCTACTCTCGCTGTCATAC
ADE2-3′	5′ ATTTACAGTTTTGATATCTTGGC 3′
ADE2-5′	5′ TTCTAATGTAGATTCTTGTTGTTCG 3′
ADE2-RIBO-3′-CA	5′ ATCGATAATACGACTCACTATAGGGTGAGTGGTTTCTAAATGTAGATTCTTGTTGTTCG 3′
ADE2-RIBO-5′-CA	5′ CTCAAATTTACAGTTTTGATATCTTGGCGT 3′
ADE2-RIBO-3′-GT	5′ GTGGTTTCTAATGTAGATTCTTGTTGTTCG 3′
ADE2-RIBO-5′-GT	5′ ATCGATAATACGACTCACTATAGGGTCAAATTTACAGTTTTGATATCTTGGCGT 3′
ADH4-HO	5′ GGAATTCTTATACTGTTGCGCGAAGTAGTCCCATAAAACTACA GCCATCATCACAAACACTGC 3′
NotI-ADH TCGGG	5′ ATAAGAATAGCGGCCGCTGTGTGGCTCATCAAAACTTCGTC 3′

10^5 cpm/ml of a probe completely internal to the Y′ element, ATTTCGGTCAGAAAGCCGGGTAAGGT.

On neutral blots, DNA in the entire lane was quantified using the PhosphorImager and ImageQuant software. For the alkaline loading control blots, only the ~1.2-kb Y′ band hybridized to the Y′-specific probe was quantified. The ratio of the neutral counts/alkaline counts was normalized with WT 0-h samples.

Flow Cytometry—Cells were processed for flow cytometry as follows: 5×10^6 cells were centrifuged and incubated in 70% ethanol. For staining, cells were centrifuged and resuspended in 50 mM sodium citrate, pH 7.4, containing RNase A (1 mg/ml) for 16 h at 50 °C. Proteinase K (1 μg/ml) was added for 1 h at 50 °C. The cells were sonicated, then incubated with 16 μg/ml propidium iodide, and analyzed with a FACSCalibur from BD Biosciences.

Okazaki Fragment Analysis at Telomeres and ARS1—Chromosomal DNA was isolated using Qiagen P20 columns. Loading buffer (6× loading buffer: 0.3 M NaOH, 6 mM EDTA, 18% Ficoll, 0.15% bromcresol green, 0.25% xylene cyanol) was added at 1× concentration to each sample. 3 μg of DNA was loaded into each well of a 1% agarose gel prepared in 50 mM NaOH, 1 mM EDTA. Electrophoresis buffer was 50 mM NaOH, 1 mM EDTA. In addition to the samples, 5′-^{32}P-end-labeled 2-log DNA ladder markers (New England Biolabs) were also loaded onto the gel. The gel was run at 30 V for 7 h with recirculation of the buffer. After electrophoresis, the gel was incubated in 0.1 M NaOH and blotted onto GeneScreen Plus with 0.1 M NaOH. 4 × 10^5 cpm/ml of the GT probe and 10^6 cpm/ml of the ARS1 probe were added to the blots in the previously described hybridization buffer. The blots were hybridized overnight at 37 °C and washed with 0.2% SSC, 0.2% SDS at 30 °C. Lagging strand at ARS1 was GCC ATG CCA AGC CAT CAC ACG GTC TTT TAT, as deduced from Bielinsky and Gerbi (63); the GT telomeric probe was TGGGTGTGGGTGTGTGTGGTGGGT.

YLpFAT10 Telomere Analysis—The YLpFAT10 parent plasmid was the kind gift of V. Zakian, and linear YLpFAT10-Tel was prepared by *in vitro* ligation of telomeric repeats onto the ends of linearized YLpFAT10 as described (64). Strains carrying the resulting linear plasmid were characterized exactly as described and then used for telomere analysis, confirming that all detectable YLpFAT10 in each strain was linear (4, 6, 64, 65). To study GT tails on linear YLpFAT10-Tel replicating *in vivo*, total genomic DNA was run on a 0.8% gel, which allows easy separation of the linear plasmid from the chromosomal DNA (5). In-gel hybridization under neutral conditions was used to detect single-stranded GT tails on YLpFAT10-Tel (5). The gel was then denatured and rehybridized as loading control. Telomere length and telomere/telomere association were estimated by cleaving YLpFAT10 with NsiI and probing with *leu2-d*, *Amp*, and/or CA-rich telomere probes, as indicated. Probes used were as follows: *AMP4,* GCA GGA CCA CTT CTG CGC TCG GCC CTT CCG GCT GGC TGG; *LEU2,* GAT GAG GCG CTG GAA GCC TCC AAG AAG GCT GAT GCC GT.

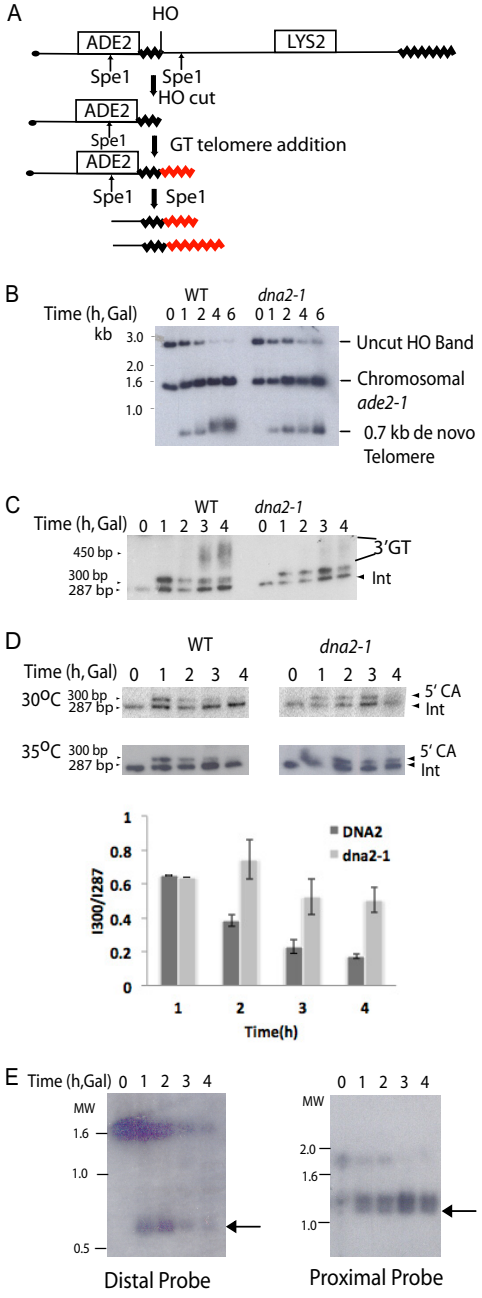

FIGURE 1. **5′-CA-strand resection and elongation of a *de novo* telomere are defective in *dna2-1* mutants.** *A*, schematic of experimental design (21). Details are found in the text. *B*, WT and *dna2-1* strains were grown in raffinose-containing media, incubated with nocodazole until 95% of the cells were arrested as dumbbells, collected by centrifugation, and resuspended in medium containing galactose to induce the HO endonuclease and nocodazole to maintain cells in G_2 phase. Cells were incubated for 0, 1, 2, 4, and 6 h at 37 °C; chromosomal DNA was isolated, cut with SpeI, electrophoresed on an agarose gel, and blotted to GeneScreen Plus, and the blot was hybridized with the *ADE2* probe. The band at about 3 kb is the SpeI fragment spanning the ADE2-HO-LYS2 construct. The ~0.7-kb fragment corresponds to the SpeI-HO cut fragment. The band at about 1.6 kb represents the endogenous *ade2-101* gene and serves as an internal standard to normalize loadings. These experiments were repeated twice with similar results. *C* and *D*, *dna2-1* cells are deficient in both 3′-GT extension and 5′-CA-strand resection at *de novo* telomeres. *DNA2* and *dna2-1* cells were grown, and the HO cut was introduced as in *B*. Cells were incubated for 0–4 h at 30 or 35 °C, as indicated. Samples were collected at each time point and harvested, and chromosomal DNA was isolated and cut with DdeI, electrophoresed on a 5% denaturing acrylamide gel, electroblotted onto a nylon membrane, and hybridized with an *ADE2* riboprobe recognizing sequences adjacent to the 3′-GT-terminated strand (*C*). The blot was stripped and then rehybridized to a riboprobe recognizing the 5′-CA-terminated strand (*D*). The DdeI-HO fragment is 300 nt. The 287-nt band below it is the internal standard corresponding to the endogenous *ade2-101* locus. *C*, 3′-GT extension is inhibited in *dna2-1*. *D*, 5′-CA-strand resection is defective. Quantification of 300-bp hybridization intensity (*Int300*) normalized to the 287-bp loading control (*Int287*) in *D* is shown in the *graph* as the mean ± S.E., $n = 2$. *E*, resection of the nontelomeric end at the *de novo* telomere is delayed. UCC5913-2-1 *dna2-1* cells were grown in raffinose-containing media at the permissive temperature, 23 °C, incubated with nocodazole until 95% of the cells were arrested as dumbbells, centrifuged, and resuspended in media containing 3% galactose and nocodazole. After incubation for an additional 0–4 h at 30 °C, nonpermissive for *dna2-1*, cells were collected; chromosomal DNA was isolated, cut with SspI, electrophoresed on a 1% agarose gel, and alkaline-blotted onto GeneScreen Plus. SspI, instead of DdeI used in *C*, is used to reveal the distal site. *Left panel,* blot was hybridized with the centromere-distal probe, a PCR product synthesized by oligonucleotides ADH4-HO and NotI-ADH4. The band disappears as resection occurs past the SspI site. *Right panel,* blot was stripped and reprobed with the proximal probe, a PCR product synthesized using oligonucleotides ADE2–3′ and ADE2–5′. The *upper band* in the doublet represents the internal *ade-102* gene, which should not change, and serves as an internal standard. The two SspI-ADE2 bands (proximal) are more difficult to separate than the two DdeI-ADE2 (proximal) bands that are seen in *C*.

RESULTS

Nuclease-defective Dna2 Is Impaired in Elongation of a de Novo Telomere—To examine the roles of nucleases in telomere synthesis, we used a strain in which telomere elongation was measured in G_2 phase cells at an HO endonuclease-induced DSB having an 81-bp telomere TG/CA seed sequence inserted centromere-proximal to the HO cut site (Fig. 1*A*) (21). The inserted TG/CA/HO sequence was flanked on the centromere-proximal side by an exogenous *ADE2* gene and on the distal side by an *LYS2* gene. Upon HO cutting, a telomerase-dependent pathway efficiently added GT/CA sequences to the telomere seed sequence (Fig. 1*B*). To monitor extension, we cut chromosomal DNA with SpeI restriction endonuclease and followed the elongation of the SpeI-HO terminal fragment by Southern blotting using a probe recognizing *ADE2*. We compared WT and the temperature-sensitive lethal *dna2-1* strain for the ability to elongate the telomere seed sequence (25). Our experiment was performed under completely nonpermissive conditions for the *dna2-1* mutants being studied (37 °C and no *HOG1* pathway inducer such as sorbitol or high salt). Telomere extension was seen in WT at 2 h and increased over the time course. Even after 6 h, little elongation is observed in *dna2-1* (Fig. 1*B*, compare *lanes 4* and *5* with *lanes 9* and *10*). We conclude that Dna2 nuclease is required for efficient telomere synthesis, as we showed previously for the *dna2-2* mutant (42), although some synthesis eventually occurs in its absence, consistent with the observations of others (58).

Nuclease-defective Dna2 Shows Impaired Resection of 5′-CA Telomeric DNA at the de Novo Telomere, and Telomeric Sequences Delay Resection at a DSB—We used the same strain to determine whether the defect in telomere elongation in the *dna2-1* mutant correlated with a defect in 5′- to 3′-CA-strand resection. After induction of the HO break, chromosomal DNA was cut with DdeI, electrophoresed on a denaturing acrylamide gel, and electroblotted. Bands were detected by hybridization with *ADE2* strand-specific RNA probes that recognized the CA or GT repeat-containing strand, respectively. The smaller band (287 bp, Fig. 1, *C* and *D*) results from hybridization to the endogenous chromosomal *ade2-101* gene, which is unaffected by HO cutting, and is a loading control. The larger band (300

bp) band appeared only after HO endonuclease induction and represented the DdeI-HO fragment containing the 81-bp telomere seed repeats. When the blot is probed with the riboprobe specific for the 3′-GT-terminating *ADE2* strand, the 300-bp band is detected at all time points, indicating that it is not degraded in either WT or *dna2-1* (Fig. 1*C*). The smear of hybridization above the 300-bp band in WT indicated that the GT-terminating strand was elongating and that, on average, 150 nt were added. The smear was absent in the *dna2-1* strain, confirming that telomere elongation is defective, consistent with the results shown in Fig. 1*B*.

When the blot is probed with the riboprobe specific for the 5′-CA-terminating *ADE2* strand, to measure resection, the 300-bp band clearly disappears over time in wild-type strains and is barely detectable at 4 h (Fig. 1*D*). In the *dna2-1* mutant, however, the CA-strand is detectable for up to 4 h, showing that resection does occur but at a dramatically reduced rate (Fig. 1*D*, *blot* and *graph*). The defect in resection occurs at 30 and at 35 °C, both of which were completely nonpermissive for *dna2-1* growth. The defect in resection of the CA-strand in the *dna2-1* mutant is similar to the defect in resection observed in the *rad50*Δ strain by Diede and Gottschling (13), and we propose that Dna2 participated in efficient CA-strand degradation. Although resection was delayed, some degradation is observed in the *dna2-1* strain at 6 h, in keeping with the results of others that a complementary, Exo1-dependent pathway exists (58).

Because it has been reported that telomeric sequences inhibit repair, resection at the centromere-distal side of the HO break, lacking telomere seed sequences, was compared in the same samples where resection on the proximal side, carrying the seed sequence, was assessed. Resection clearly occurred more efficiently on the distal terminus lacking the 81-bp telomeric repeat sequence (Fig. 1*E*, compare *1-* and *2-h time points*), demonstrating that the telomeric sequences give rise to a structure that inhibits telomeric end processing in the G_2 phase of the cell cycle, as has been shown previously in wild-type cells (21). Similar inhibition of repair of a DSB by telomeric sequences has recently been noted for nonhomologous end joining in G_1 phase yeast cells and in mammalian cells (66).

dna2 Mutants Are Defective but Not Blocked in GT-overhang Production in S Phase at Native Telomeres—The *de novo* telomere is a model for the blunt-ended leading strand telomere. It was generated in G_2, after DNA synthesis was complete, and had only a 4-bp 3′-overhang. The *de novo* telomere sequence used here was 81 bp, about 200 bp shorter than a native telomere. We wondered if Dna2 was also required at native telomeres in S phase, which was when long replication-associated GT-overhangs appeared, and if Dna2 was required for both leading and lagging strands. We therefore monitored the appearance of telomere 3′-GT-overhangs on native chromosomal telomeres in cells undergoing a synchronous cell cycle. For these experiments, we used a *dna2*Δ mutant, and thus all strains, except the wild-type (WT) control, contain a *pif1*Δ mutation, which suppresses the lethality of *dna2*Δ (53).

Cells were arrested with α factor and then released into the cell cycle at 30 °C, a semi-permissive temperature. At various times after release, DNA was purified and cut with XhoI, which cleaves Y′-containing telomeres ~1.2 kb from the end (67), yielding terminal fragments differing in length only by the extent of telomeric tracts (Fig. 2*A*). Subtelomeric Y′ elements were found in about half of all yeast telomeres, depending on the strain. Neutral Southern blotting was performed with a telomere-specific CA-rich oligonucleotide probe to detect single-stranded GT DNA. Fig. 2*A* shows the time course of appearance of single-stranded GT DNA as G_1 cells enter and traverse the S phase after α factor release. The position of the Y′-telomere population was indicated. The hybridization signals extending upward from the ~1.2-kb region represent overhangs on the yeast telomeres that lack Y′ elements and therefore have longer heterogeneous XhoI terminal fragments. A loading control is shown (Fig. 2*A*, *DENATURED,* which also indicates relative telomere length). In-gel hybridization resulted in large losses of DNA in the critical 1-kb range in our hands, accounting for the use of the more cumbersome but more quantitative blotting methods described here.

In wild-type G_1 cells, we observed no long GT-overhangs (0 min) by this method, as shown previously. Unlike the *de novo* telomere in *dna2-1* mutants, elongated 3′-GT-overhangs were detected at 45 min in all strains, including *dna2*Δ *pif1*Δ (Fig. 2*A*, *lanes 3, 6,* and *9*). At this time point, all strains were in S phase as determined by flow cytometry. The apparent delay in the *dna2*Δ *pif1*Δ strain was not reproducible (see Fig. 3) and coincided with a delay in the cell cycle (data not shown). The single-stranded DNA is at the terminus and is not internal, because, in a second experiment (Fig. 2*B*), treatment of samples before electrophoresis with bacterial exonuclease 1, which degrades ssDNA from 3′-OH termini, eliminated the 3′-GT signal in all of the strains at all S phase time points. Quantification (data not shown) by normalizing the signals in Fig. 2, *A* and *B*, *NATIVE*, to the loading controls, *DENATURED*, indicated that 3′-GT tails appear only moderately, if at all, at reduced levels in *dna2*Δ *pif1*Δ compared with *pif1*Δ strains. From these data, it was clear that Dna2 was not exclusively required for resection, but it was not clear whether the slight reduction was significant.

3′-GT-overhangs are not detected in telomere blots of wild-type strains in G_1 (4), but we noticed a reproducible G_1 phase population of long chromosomal 3′-GT tails in the *pif1*Δ mutants. As reported previously, this G_1 population is not apparent in our wild-type control strain (Fig. 2*A*, compare *lane 1* with *lane 4* and with *lane 7*). The detection of single-stranded DNA in G_1 may be due to the fact that *pif1*Δ strains contain inherently longer telomeres than wild type, and telomere length is known to regulate resection (68). Although the GT-overhangs increase over the G_1 level during S phase in the *pif1*Δ mutants (Fig. 2*A*, *lanes 5* and *6*), just as they do in wild type, we were concerned that the overhangs observed in *dna2*Δ *pif1*Δ might only be found in the absence of Pif1.

To determine whether GT-overhangs arise at native telomeres in the absence of Dna2 when Pif1 helicase was present, we repeated our studies in a different strain background. We used a *dna2*Δ *rad9*-null (*rad9-320*) mutant. We have shown that *rad9-320*, a *rad9* mutation with a stop codon at amino acid 320, which was null for essential Rad9 functions, suppresses the inviability of *dna2*Δ (69). As shown in Fig. 2, *C* and *D*, as in wild type, these strains lack overhangs in G_1. Overhangs lengthened in S phase in all strains, including *dna2*Δ *rad9-320*. Thus, the

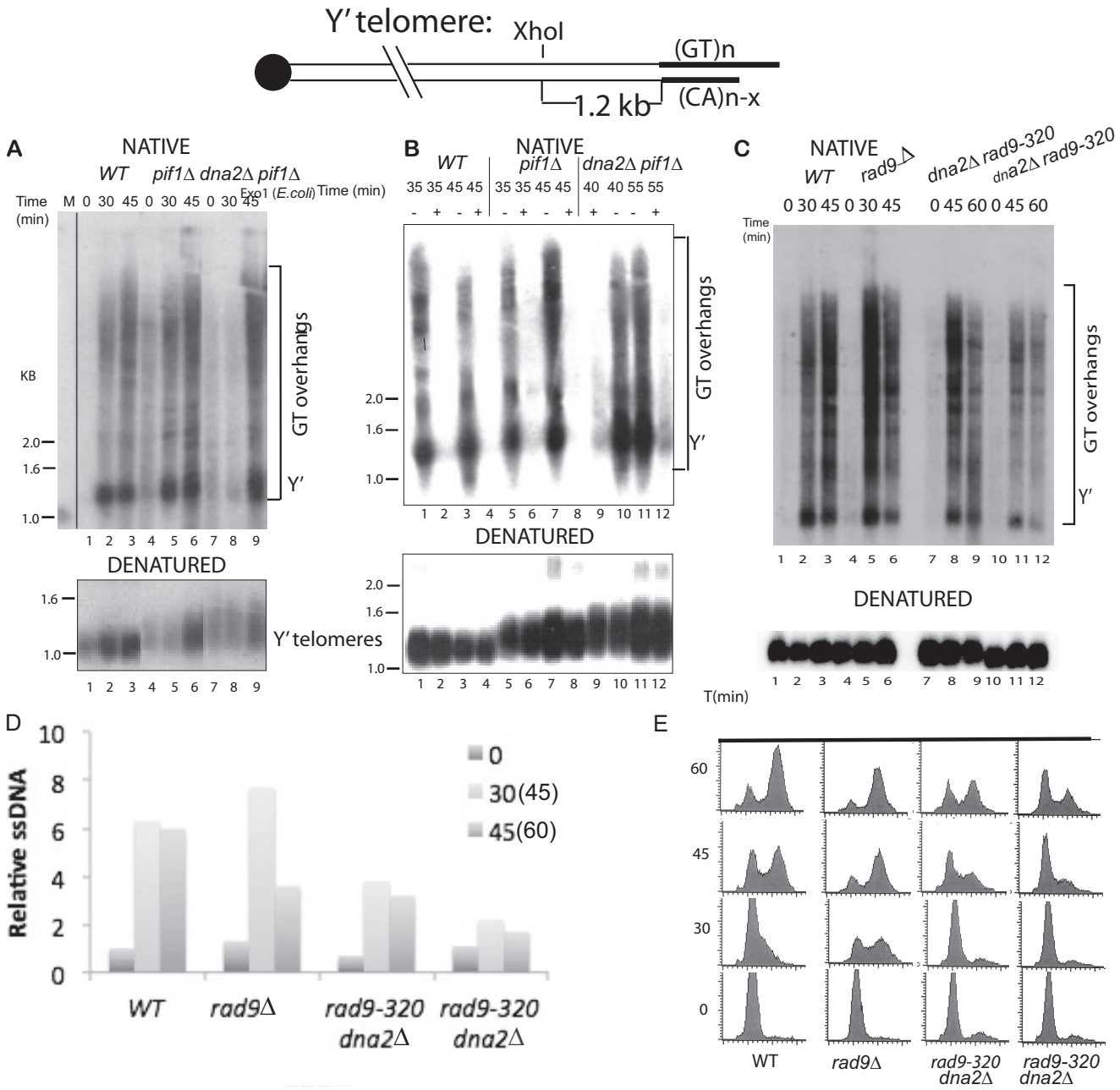

FIGURE 2. **Analysis of single-stranded GT-overhangs at native telomeres in *dna2*Δ strains.** *A,* schematic of Y′ telomere. *B,* determination of overhang extension in S phase. WT (BY1408), *pif1*Δ (MB121), and *dna2*Δ *pif1*Δ (MB161B) were grown at 30 °C, arrested with α factor, and then released into a synchronous cell cycle. Samples were taken at 0, 30, and 45 min after release. DNA was prepared and cleaved with XhoI to release terminal fragments. The fragments were separated by gel electrophoresis and blotted to GeneScreen Plus under neutral/*NATIVE* conditions as described under "Experimental Procedures." The blots were probed with a telomere-specific CA-rich oligonucleotide probe, which detects GT-overhangs. All samples were from the same gel but were rearranged in Photoshop for logical presentation. Notice, for instance, seam between samples 5 and 6 and 6 and 7. *DENATURED*, the same samples (0.1 volume) were analyzed after alkaline blotting as a loading control for XhoI-cut DNA. Only the terminal ~1.2-kb XhoI fragments (*i.e.* from Y′ telomeres) are shown. Gels were not run long enough to determine telomere length differences in the respective strains. These experiments were repeated three times with the same result. (Flow cytometry of these strains is shown in Fig. 3, *C* and *D*). *B,* single-stranded DNA is at the telomere termini and is not internal. Analysis of XhoI-cut DNA from synchronized S phase cells was after cleavage with *Escherichia coli* 3′-exonuclease I. *NATIVE,* cells were arrested with α factor and released into the cell cycle. S phase samples with GT-overhangs were taken from WT and *pif1*Δ cells at 35 and 45 min, and samples were taken from *dna2*Δ *pif1*Δ at 40 and 55 min to account for the slower progression through the cell cycle of the double mutant. XhoI-digested DNA samples were divided in half, and one-half was treated with bacterial exonuclease 1 as described under "Experimental Procedures." Samples were then analyzed by neutral blotting as in *A* (*NATIVE*). *DENATURED*, loading control. The same samples (0.1 volume) were analyzed after alkaline blotting. Note that the gel was not run long enough to provide sufficient resolution to estimate telomere length in the mutants, which we have reported previously. *C, dna2*Δ *rad9-320* strains are defective in producing long single-stranded overhangs at native telomeres. The experiment was performed as described in *A* and *B*. The *NATIVE* gel was hybridized to the CA probe. The *DENATURED* loading control was hybridized to a Y′-specific probe to avoid differences in signal due to different telomere lengths in the various strains. The amount of single-stranded DNA was normalized to the loading control and zero time point. *D,* quantification of data in *C*. Note that *lanes 10–12* are a repeat of *lanes 7* and *8* using a different clone of the same strain and show similar results. *E,* flow cytometry of samples analyzed in *C* and *D*.

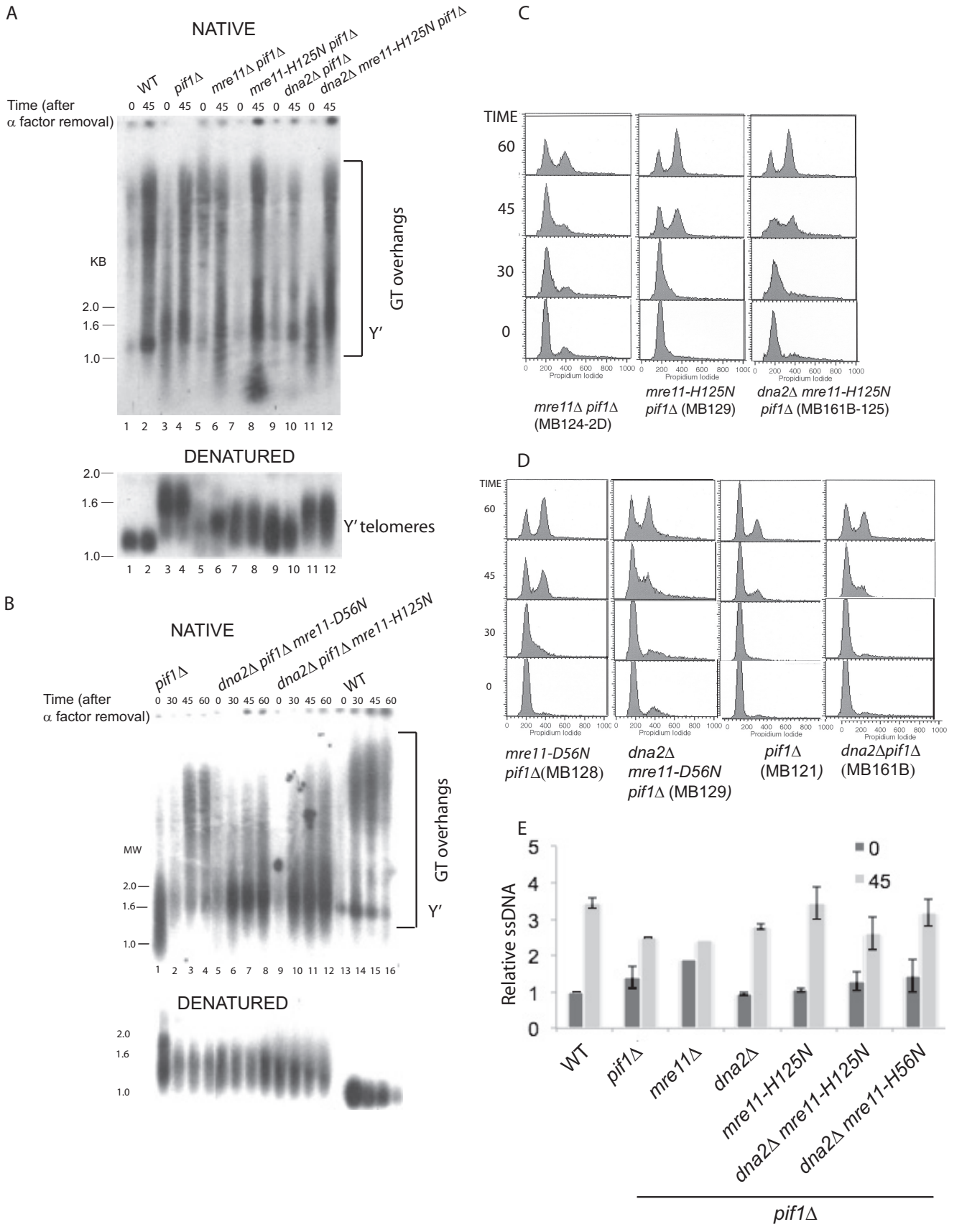
A
NATIVE
WT
pif1Δ
mre11Δ pif1Δ
mre11-H125N pif1Δ
dna2Δ pif1Δ
dna2Δ mre11-H125N pif1Δ
Time (after α factor removal)
0 45 0 45 0 45 0 45 0 45 0 45
KB
2.0
1.6
1.0
GT overhangs
Y′
1 2 3 4 5 6 7 8 9 10 11 12
DENATURED
2.0
1.6
1.0
Y′ telomeres
1 2 3 4 5 6 7 8 9 10 11 12
B
NATIVE
pif1Δ
dna2Δ pif1Δ mre11-D56N
dna2Δ pif1Δ mre11-H125N
WT
Time (after α factor removal)
0 30 45 60 0 30 45 60 0 30 45 60 0 30 45 60
MW
2.0
1.6
1.0
GT overhangs
Y′
1 2 3 4 5 6 7 8 9 10 11 12 13 14 15 16
DENATURED
2.0
1.6
1.0
C
TIME
60
45
30
0
0 200 400 600 800 1000
Propidium Iodide
mre11Δ pif1Δ (MB124-2D)
mre11-H125N pif1Δ (MB129)
dna2Δ mre11-H125N pif1Δ (MB161B-125)
D
TIME
60
45
30
0
0 200 400 600 800 1000
Propidium Iodide
mre11-D56N pif1Δ(MB128)
dna2Δ mre11-D56N pif1Δ (MB129)
pif1Δ (MB121)
dna2Δpif1Δ (MB161B)
E
Relative ssDNA
0
1
2
3
4
5
0
45
WT
pif1Δ
mre11Δ
dna2Δ
mre11-H125N
dna2Δ mre11-H125N
dna2Δ mre11-H56N
pif1Δ

absence of Pif1 was not responsible for the appearance of GT-overhangs in *dna2*Δ *pif1*Δ. Although overhangs occur in the absence of Dna2, we found a reproducible 2-fold reduction in GT-overhangs in *dna2*Δ *rad9-320* strains compared with wild type or *rad9*Δ. Also shown is the fact that the *rad9*Δ and the *dna2*Δ *rad9*-null double mutant telomeres, unlike *dna2*Δ *pif1*Δ telomeres, are the same length (Fig. 2*C,* mutant 1, *lanes 7–9*) or shorter than in WT (Fig. 2*C,* mutant 2, *lanes 10–12*), suggesting *rad9*Δ does not affect telomeres. Although it has never been directly demonstrated, it is generally and reasonably accepted that the reduction in GT-overhang signal corresponded to shorter overhangs and therefore to a defect in resection of the 5′-CA-strand. Therefore, we conclude that Dna2 participates in one resection pathway at native telomeres, just as has been shown for its partner Sgs1 helicase (58), but that other pathways must also exist and can more efficiently compensate for loss of Dna2 at native telomeres than at the short *de novo* telomere.

Interaction of Dna2 and Mre11 Nuclease at Native Telomeres—Because Mre11 nuclease is required for resection of x-ray-induced DSBs in the absence of Dna2 and vice versa (46), we expected that a *dna2*Δ *mre11-nuclease minus* double mutant would have a greater defect in formation of GT-overhangs than *dna2*Δ. Mre11, the nuclease component of the Mre11 Rad50 Xrs2 (MRX) complex, was one of the nucleases creating 3′-GT-overhangs. MRX deletion mutants have very short telomeres with abnormally short GT-overhangs (5, 12, 60). MRX is associated primarily with leading strand telomeres (5, 9, 13). MRX is required for an early step in processing of DNA DSBs at internal chromosomal loci (45, 61). Even though the MRX exonuclease has 3′ to 5′ directionality, rather than the expected 5′ to 3′ activity, MRX can support resection in the 5′ to 3′ direction, either by forming a hairpin and using its associated endonuclease activity or as a bidirectional nuclease reaction involving both MRX endonuclease, exonuclease, and Dna2 or Exo1 5′-exonuclease (70, 71). The N terminus of Mre11 contains the phosphodiesterase active site of both the endonuclease and 3′- to 5′-exonuclease of Mre11 (71–74). Mutations *mre11-D56N* and *mre11-H125N* each inactivate both endo- and exonuclease activities and result in a strain with mild sensitivity to DNA-damaging agents but no shortening of the telomere nor defects in the lengthening of 3′-GT-overhangs during S phase (75). This implies that other nucleases, such as Dna2, also participate.

The appearance of 3′-GT-overhangs was investigated in the *dna2*Δ *mre11-nuclease minus pif1*Δ mutant. (We have not been able to construct a viable *dna2*Δ *mre11-nuclease minus rad9-320* mutant.) As shown in the *NATIVE* blot in Fig. 3, 3′-GT-overhangs increase in S phase in two independent *dna2*Δ *mre11-nuclease minus pif1*Δ triple mutants (Fig. 3, *A, lanes 11* and *12,* and *B*, *lanes 6–12*), just as they do in wild-type, single, and double mutant strains (Fig. 3*A*, *lanes 1–10*). (Flow cytometry profiles are shown in Fig. 3, *C* and *D.*) The normalized amounts of S phase-overhangs in *dna2*Δ *mre11-D56N pif1*Δ were similar to those in the *dna2*Δ *pif1*Δ, and inactivation of Mre11 nuclease did not abolish resection. Although GT-overhangs are detectable in G_1 phase, it is significant that the GT-overhang signal increases from G_1 into S phase in the *dna2*Δ *mre11-D56N pif1*Δ and *dna2*Δ *mre11-H125*N *pif1*Δ strains as it does in wild-type cells (Fig. 3, *A*, *B* and *E*). When the native blots were hybridized with a probe complementary to the Y′/GT boundary, no signal was observed, showing that the 3′ ssDNA did not extend into the Y′ region (data not shown). Results are quantified in Fig. 3*E*, verifying that overhangs are not only present in *dna2*Δ *mre11-nuclease minus* but that they are longer than in *dna2*Δ. The presence of 3′-overhangs in a *dna2*Δ *mre11-nuclease-minus* strain was completely unexpected, especially because such mutants were completely defective in DSB repair. The differences in Y′-telomere lengths revealed in the alkaline blot of the same samples is a subject for further study (Fig. 3, *A* and *B*, *DENATURED*).

Exo1 was also redundant with Dna2 in resection at intrachromosomal DSBs. We were unable to construct a viable *dna2*Δ *exo1*Δ *pif1*Δ much less a *dna2*Δ *exo1*Δ *mre11-H125N pif1*Δ mutant, presumably because such mutants were inviable, and we could therefore not evaluate GT-overhangs in a triple nuclease-deficient mutant.

Analysis of Telomeres on Linear Plasmids in dna2 mre11 Mutants—To confirm the unanticipated ability of *dna2*Δ and *mre11-nuclease minus* mutants to produce long 3′-overhangs, we used the linear plasmid YLpFAT10-Tel (64). This short linear plasmid has normal length telomeres, replicates to high copy number, and acquires terminal GT-tails $>$ 30 nt in length in late S phase, retaining shorter tails even in G_1 phase (4–6, 65). As such, YLpFAT10 offers a higher sensitivity and a higher resolution adjunct to the chromosomal telomere blot data in Fig. 3. We compared telomere overhangs on YLpFAT10 grown in *mre11*-nuclease *minus*, *dna2*Δ, and *mre11-nuclease minus dna2*Δ double mutant strains. All of these mutants were in a *pif1*Δ background. Synthetic telomeres were ligated onto YLpFAT10 *in vitro*; the plasmids were introduced into the various mutant strains, and transformants carrying unit length and linear YLpFAT10-Tel of ~8–9 kb were identified as described previously (data not shown) (6). Fig. 4*A* shows a schematic of YLpFAT10-Tel. Because YLpFAT10-Tel is greater than 8 kb in length but is well separated from chromosomal DNA upon gel electrophoresis, in-gel hybridization was used to monitor single-stranded telomeric tails (and telomere length) (6). Respective YLpFAT10-Tel transformants were synchronized with α factor (0 min) and released into S phase for 45 min. Plasmid DNA was analyzed at both time points (Fig. 4*B*, *odd-numbered lanes*, α factor; *even-numbered lanes*, S phase). As on chromosomes, single-stranded GT tails arose in *pif1*Δ strains both in

FIGURE 3. ***dna2 mre11-nuclease-deficient*** **double mutants are not defective in production of single-stranded DNA in S phase at native telomeres.** *A, top panel,* indicated strains were grown at 30 °C, arrested with α factor, and released into the cell cycle as described under "Experimental Procedures." Samples were collected at the times indicated, cleaved with XhoI, and analyzed by neutral blotting for single-stranded DNA (*NATIVE*) and alkaline blotting as a loading control (*DENATURED*) as described in Fig. 2 and under "Experimental Procedures." Hybridization was carried out with the same probe for both gels. *B,* indicated strains were treated as in *A*. *C* and *D,* flow cytometric analysis of cell cycle progression of strains used in *A* and *B*. *E,* quantification of overhang data, mean ± S.E., $n = 3$ for WT, *dna2*Δ *pif1*Δ, *dna2*Δ *pif1*Δ *mre11-H125N*; $n = 2$ for *pif1*Δ *dna2*Δ *mre11-H56N*. The amount of single-stranded DNA in each was normalized to the loading control rehybridized with a Y′-specific probe. Normalization was to 0 time.

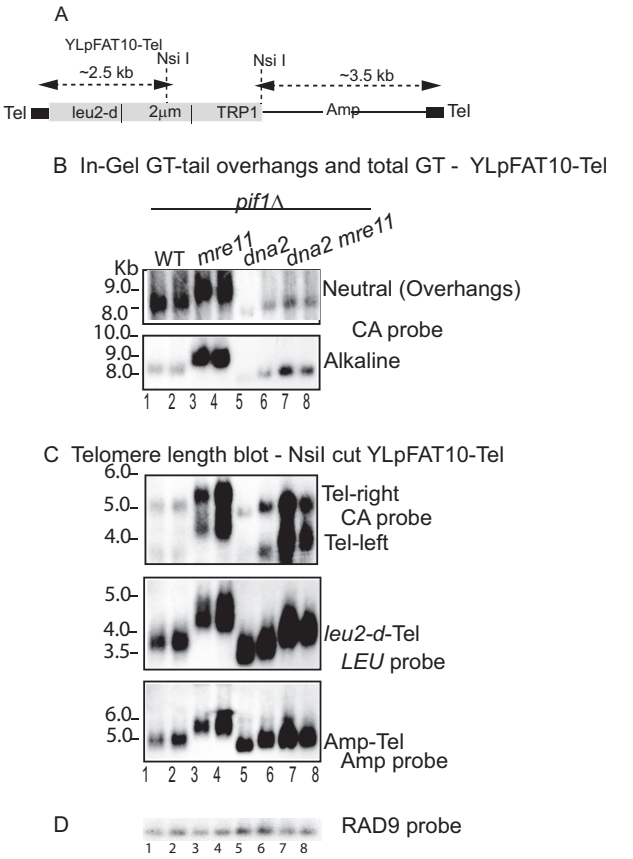

FIGURE 4. **Long GT-overhangs appear in S phase on linear YLpFAT10-TEL in *dna2*, *mre11-nuclease minus*, and in *dna2 mre11-nuclease minus* double mutants.** *A*, schematic map of YLpFAT10-Tel, about 7.5 kb plus the length of the telomeric repeats. *B*, overhangs on YLpFAT10-Tel. The respective strains carrying linear YLpFAT10 were grown at 30 °C, arrested with α factor, and released into the cell cycle for 45 min. *Upper panel*, genomic DNA was isolated and separated on a neutral gel. In-gel hybridization with the CA probe hybridizing to GT-overhangs was carried out as described (6). The gel was then soaked in NaOH to denature the DNA and, after neutralization, rehybridized with the CA probe to determine the total GT DNA. *Lanes 1* and *2*, *MRE11 DNA2 pif1*Δ, 0 and 45 min after release from α factor; *lanes 3* and *4*, *mrell-H125N pif1*Δ, 0 and 45 min; *lanes 5* and *6*, *dna2*Δ *pif1*Δ, 0 and 45 min; *lanes 7* and *8*, *mre11-H125N dna2*Δ *pif1*Δ, 0 and 45 min. *C*, to estimate telomere length and to monitor telomeric DNA on both ends of the plasmid, the same samples were cut with NsiI and separated by gel electrophoresis. Southern blots were hybridized with the CA oligonucleotide (*top panel*). The blot was then washed and rehybridized with a *LEU2* probe to the 2.5-kb end as loading control, copy number control, and length control (*middle panel*). Finally, the blot was washed and hybridized to the *AMP4* probe to confirm the 3.5-kb end (*bottom panel*). *Lanes 1* and *2*, *pif1*Δ, 0 and 45 min after release from α factor; *lanes 3* and *4*, *mrell-H125N pif1*Δ, 0 and 45 min; *lanes 5* and *6*, *dna2*Δ *pif1*Δ, 0 and 45 min; *lanes 7* and *8*, *mre11-H125N dna2*Δ *pif1*Δ, 0 and 45 min. These experiments were duplicated (using independent transformants) with the same quantitative results for GT-overhangs, steady-state GT tract length, and steady-state plasmid copy number. *D*, loading control from chromosomal DNA for *C*. The blot shown in *C* was hybridized to a *RAD9* probe to normalize for single copy DNA content.

G_1 and in S phase. More importantly, single-stranded GT tails arose on YLpFAT10-tel, not only in *MRE11 DNA2* wild type (Fig. 4*B*, *lanes 1* and *2*) and in the *mre11-H125N* or *dna2* single mutants (Fig. 4*B*, *lanes 3* and *4* and *5* and *6*, respectively) but also in *dna2 mre11-H125N* double mutants (Fig. 4*B*, *lanes 7* and *8*). Thus, the overhangs in the *dna2* mutant were not arising because Mre11 nuclease is a backup for Dna2 or vice versa. We also noted that just as overhangs at chromosomal telomeres were shorter in *dna2*Δ *rad9*Δ than in *rad9*Δ, plasmid telomere overhangs were shorter in *dna2* Δ *pif1*Δ than in *pif1*Δ. Normalized results of overhang length measurement are presented

TABLE 2
Overhangs on YLpFAT10-tel in *pif1*Δ *dna2*Δ and *pif1*Δ *dna2*Δ *mre11-125*
ND = not determined.

Strain	Min	Exp. 1	Exp. 2
*pif1*Δ	0	1[a]	1
*pif1*Δ	45	0.75	0.73
*pif1*Δ*mre11-125*	0	ND	0.70
*pif1*Δ *mre11-125*	45	ND	0.38
*pif1*Δ *dna2*Δ	0	0.53	0.06
*pif1*Δ *dna2*Δ	45	0.56	0.09
*pif1*Δ *dna2*Δ *mre11-125*	0	0.56	0.06
*pif1*Δ *dna2*Δ *mre11-125*	45	0.49	0.06

[a] The phosphorimager counts in the neutral gel (Fig. 4*B*) were divided by the LEU2 counts or by the Amp counts (Fig. 4*C*) for each strain. The average of the two results was normalized to the average for the *pif1*Δ strain at 0 min and are the values reported.

numerically in Table 2. These observations indicate that resection nucleases indeed interact differently at telomeric repeats than at intra-chromosomal DSBs (Figs. 3, *A* and *B*, and 4). These observations suggest that other nucleases, Exo1 or others, are efficient in producing telomere overhangs in the absence of both Dna2 and Mre11.

We noticed a difference in intensity of the GT hybridization among the strains. This difference was also observed after denaturation of the gel and rehybridization with the CA probe. The difference in hybridization was not accounted for by YLpFAT-10-tel copy number, because hybridization with YLpFAT-10-tel internal *LEU2* or ampicillin probes did not differ to the same degree, and loading of chromosomal DNA was approximately equivalent among the strains (Fig. 4, *C* and *D*). These results suggested that the difference in intensity of bands in Fig. 4 reflects the amount of GT/CA tract present on the plasmids, *i.e.* the equilibrium telomere length attained in each mutant. To estimate total G-tract length directly, the same DNA samples were treated with NsiI, which produces one terminal ~2.5-kb YLpFAT10 fragment containing the *leu2-d* gene and a second terminal ~3.5-kb fragment carrying the *Amp* resistance gene (see Fig. 4*A*). After gel electrophoresis and Southern blotting, both the ~2.5- and ~3.5-kb fragments reveal terminal GT tracts (Fig. 4*B*, *CA probe*). The length of these restriction fragments differ in plasmids from the different strains, indicating the difference in the steady-state length of the telomeres (Fig. 4*B*, LEU2 and AMP4 probes). *pif*Δ *dna2*Δ had shorter telomeres than *pif1*Δ, as in Fig. 3 and as we have shown previously. *pif1*Δ *dna2*Δ *mre11-H125N* also carried shorter telomeres than *pif*Δ. The YLpFAT10 telomeres appear very long (>1 kb) compared with the native Y′ telomeres (<0.5 kb) (compare Figs. 4*C* with 3, *A* or *B*, *DENATURED*). This significant derepression of YLpFAT10 telomere length may suggest that the high density of nucleosomes at Y′ regions negatively regulates telomere length (76).

GT-overhangs Also Accumulate in Mutants Lacking Both Dna2 and Exo1—At *de novo* telomeres, Exo1 (yeast exonuclease 1) can compensate for loss of Dna2 in long range resection (58), but this has not been investigated at native telomeres. Because *dna2*Δ *exo1*Δ is inviable even in *pif1* or *rad9* backgrounds, we used *dna2-2* mutants for this experiment. We chose *dna2-2*, because *dna2-2*, like *dna2-1* (Fig. 1), is defective in *de novo* telomere elongation (42), but *dna2-2 exo1*Δ mutants grow much better than *dna2-1 exo1*Δ mutants. To ensure good

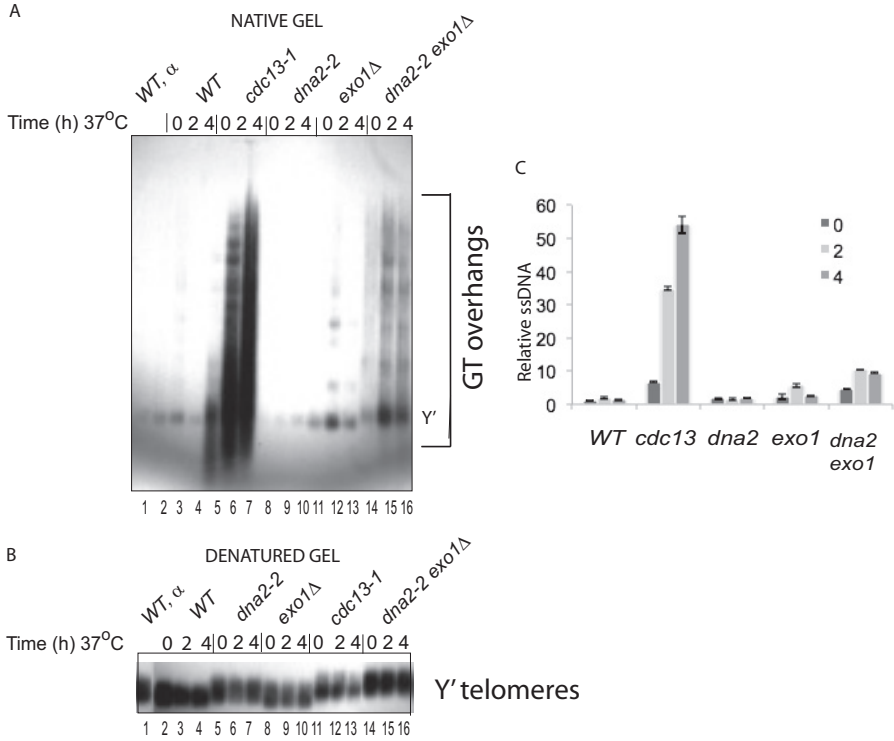

FIGURE 5. ***dna2 exo1* mutants accumulate single-stranded DNA in S phase at native telomeres.** Analysis of XhoI cut DNA from asynchronous cells. *NATIVE*, wild type (MB214), *cdc13-1* (MB215), *exo1*Δ (MB216), *dna2-2* (MB214), and *dna2-2 exo1*Δ (MB217) were grown to log phase in medium containing 0.5 M sorbitol, which is essential to allow growth of the *dna2-2 exo1*Δ mutant and shifted to 37 °C for the indicated times (0, 2, or 4 h) in the absence of sorbitol. DNA was prepared, and GT-overhangs were analyzed on neutral agarose gels as described under "Experimental Procedures" and the legends to Figs. 2 and 3. *DENATURED,* the same DNA samples were analyzed on a separate gel, which was blotted under denaturing conditions. The experiment shown is a representative example of three biological replicates showing similar results. Quantification of the experiment shown is at the *right*. The mean of normalization to two different Y′ bands, one at 1.2 kb, is shown, and another at 6.5 kb (data not shown) is found in this strain using the Y′-specific probe.

growth, we propagated *dna2-2 exo1*Δ on medium or high osmotic strength 0.5 M sorbitol (77), which induces Hog1 stress response kinase that stabilizes replication forks experiencing replication stress (78). Suppression of growth defects by sorbitol was not complete, because *dna2-2 exo1*Δ cells were temperature-sensitive (37 °C) for growth on sorbitol-containing medium. All strains were nevertheless shifted to glucose upon shift to 37 °C. GT-overhangs were difficult to detect in asynchronously cycling wild-type cells but accumulated in temperature-sensitive *cdc13-1* mutants when they were shifted to 37 °C, where uncapping occurred due to the temperature-sensitive single-stranded GT-DNA-binding protein, Cdc13. Therefore, GT-overhangs of wild type and *cdc13-1* were compared, as negative and positive controls, to GT-overhangs in the *dna2-2 exo1*Δ mutant (Fig. 5*A*). When WT, *dna2-2,* or *exo1*Δ strains were shifted to 37 °C, there was no or little accumulation of long single-stranded GT-overhangs (Fig. 5*A*, *lanes 4–11*). When *dna2-2 exo1*Δ double mutants were incubated at 37 °C, however, an increase in single-stranded GT-overhangs was observed (Fig. 5, *A*, *lanes 15* and *16,* and *B*, loading controls, and *C*, quantification). A role in resection should have led to a decrease rather than an increase in GT-overhang. The increase in GT-overhangs is similar to what has been observed in *rad27*Δ mutants, lacking FEN1, where long single-stranded G tails accumulate even though FEN1 is not required for telomere overhang generation by resection (79). Given the role of FEN1 in Okazaki fragment maturation, our results suggested to us that GT-overhangs might increase in *dna2-2 exo1*Δ mutants due to a failure of the lagging strand replication apparatus to complete the CA-rich, discontinuously replicated strand (CA-strand fill-in). The *dna2-2 exo1*Δ telomeres are also significantly longer than those in wild type (Fig. 5*B*). This phenotype is also similar to that seen in polα mutants (80, 81) and therefore could be due either to a defect in joining of replication intermediates or a defect in fill-in synthesis by polymerase.

Dna2 Is Required for Efficient Nascent Strand Maturation at Native Telomeres—Single-stranded DNA can in principle occur at telomeres due to a failure to complete replication of the lagging strand template (either before or after telomerase action) or due to the uncontrolled resection of ends at uncapped telomeres. The unexpected appearance of extended DNA overhangs at native telomeres in *dna2-2 exo1*Δ mutants prompted us to look directly for enhanced accumulation of lagging strand-specific, low molecular weight, nascent replication intermediates (RIs) at telomeres in *dna2* mutants. To establish that we could see nascent intermediates likely to reflect inhibition of lagging strand processing, we used a *cdc9-1* and a *cdc9-1 rad9*Δ double mutant. The *rad9*Δ checkpoint mutation allows for more complete replication of the genome in S phase and was used to ensure that telomeres, which replicate late in S phase, actually underwent DNA replication (82, 83). DNA was isolated from *cdc9-1* or *cdc9-1 rad9*Δ cells that had been synchronized with α factor, released at 36 °C, and then allowed to pass through S phase at the nonpermissive temperature. We used alkaline gels and Southern blotting to identify replicative intermediates at telomeres, using a GT-rich telomere-specific probe

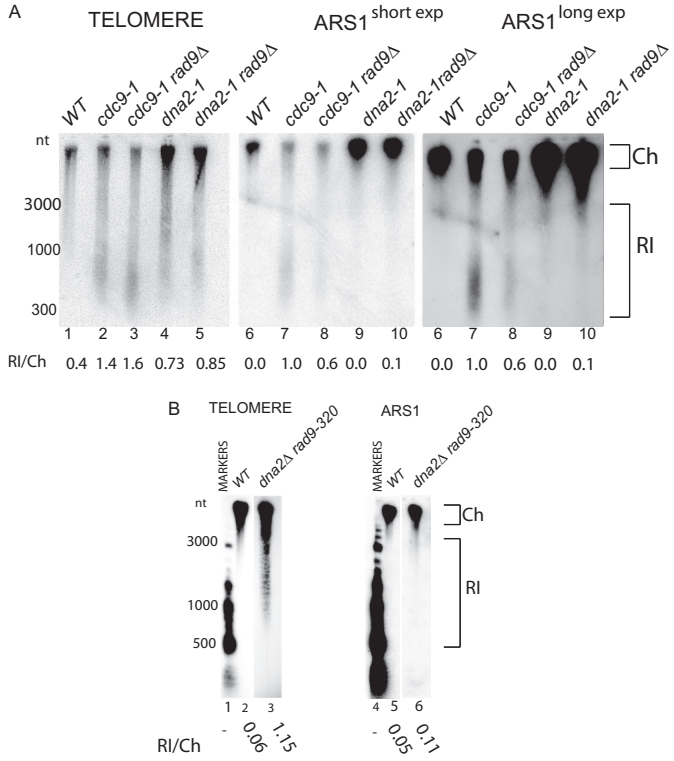

FIGURE 6. **Both *dna2-1* and *dna2*Δ *rad9-320* mutants are defective in nascent DNA maturation at telomeres.** *A,* comparison of nascent telomeric DNA in *cdc9-1* and *dna2-1* mutants. Wild type, *cdc9-1*, or *cdc9-1 rad9*Δ mutants were synchronized with α factor and released into S phase for 45 min (*WT*) or 60 min (*cdc9-1* and *cdc9-1 rad9*Δ) at 36 °C. Genomic DNA was isolated and subjected to alkaline gel electrophoresis to release newly synthesized DNA. Nascent DNA was identified with a telomeric probe (*left panel*) or an *ARS1* probe (*right panel*), specific for the lagging strand at *ARS1*, after Southern blotting. The telomere-specific probe was GT-rich, because the nascent DNA from the lagging strand is CA-rich. Ch marks chromosomal sized DNA, and RI indicates DNA shorter than 3 kb. *dna2-1* and *dna2-1 rad9*Δ mutant strains were released from α factor and grown for 60 min at 36 °C before DNA isolation to allow for their slower cell cycle progression. Blots were hybridized to telomere-specific GT probe (*left panel*) or ARS1 lagging strand probes (*middle* and *right panels*). These experiments were repeated at least once with similar results. The RI/Ch ratio, reported below the blots, was determined as described in the text, and the values reported are the average of several experiments (*lane 1*, $n = 1$; *lane 2*, $n = 1$; *lane 3*, $n = 2$; *lane 4*, $n = 2$; *lane 5*, $n = 2$. *B, dna2*Δ mutants are defective in nascent DNA maturation at telomeres. The indicated strains were grown at 30 °C after α factor release but were otherwise treated as in *A* and probed with a telomeric GT-rich probe. *Left panel, lanes 1–3*, or an *ARS1* lagging strand probe; *right panel, lanes 4–6*. Results are the average of $n = 2$.

that hybridizes to the CA-rich, discontinuously synthesized DNA. We then reprobed the same blot with a lagging strand oligonucleotide from *ARS1*, representing an early firing internal origin of replication, for comparison. We observed short lagging strand fragments, both within the telomeric repeats and at *ARS1* (Fig. 6*A*, *lanes 2* and *3* and *7* and *8*). This method can therefore detect nascent DNA both at telomeres and at internal sites. The RIs at *ARS1* are of a discrete size compared with a broader size distribution that is reproducibly observed at telomeres, possibly attributable to the nucleosome-free nature of telomeric repeats (83). The intermediates at *ARS1* are the same length as observed previously (84) but are slightly longer than the monomeric Okazaki fragments recently described (83), which is probably explained by the fact that the recent study used a more stringent Cdc9 shutoff, *i.e.* transcriptional repression and degron induction.

We then carried out the same experiment in *dna2-1* and *dna2-1 rad9*Δ strains. *dna2-1* contained a P504S mutation in the nuclease domain that severely inhibited both the intrinsic nuclease and the helicase/ATPase and is temperature-sensitive for growth even at 28 °C. Cells were released from G_1 arrest into S phase at 36 °C for 55 min. To quantify the efficiency of converting the RIs into chromosomal sized DNA, the counts in DNA that were 2.5 kb or smaller in size were determined using the PhosphorImager and ImageQuant software. This size range was chosen because it is even smaller than the size reported previously for nascent DNA in a similar analysis of RIs at ARS1 in the presence of hydroxyurea (84). To normalize results in the different strains, the RIs in each lane were divided by the counts from the chromosomal region (Ch) of the lane, and the RI/Ch ratio is reported below each lane. (Similar relative amounts were obtained if RIs smaller than 5 kb were quantified.) Wild-type strains efficiently ligated nascent chains at *ARS1*, although the efficiency of ligation in this experiment appeared reduced at the telomere. The accumulation of RIs at telomeres in *dna2-1* and *dna2-1 rad9*Δ mutants at telomeres was slightly, although reproducibly, greater than wild-type cells (Fig. 6*A*, *lanes 1, 6,* and *11*). At *ARS1*, *dna2-1* mutants were nearly as proficient as wild-type cells at converting RIs into chromosomal sized fragments. The *ARS1* hybridization establishes that the single-stranded DNA observed at telomeres was not due to DNA degradation during sample preparation.

Because Dna2 is partially functional in *dna2-1* mutants, which might account for the high level of residual RI maturation, we next assayed the ability of *dna2*Δ strains to join nascent fragments at telomeres and ARS1, using the *dna2*Δ *rad9-320* strain employed in the experiment in Fig. 2. In Fig. 6*B*, we compared wild type and *dna2*Δ *rad9-320* mutants for nascent fragment maturation. At telomeres, the defect in joining nascent fragments in *dna2*Δ *rad9-320* was almost as severe as in *cdc9-1* (compare Fig. 6, *A* and *B*). The defect in *dna2*Δ *rad9-320* was slightly less than in *cdc9* mutants, as expected because reduction of Dna2 may delay the maturation of RIs into chromosomal sized fragments, but it is not expected to result in fragments as short or long lived as observed in *cdc9* mutants, due to redundancy of Dna2 with Exo1 or FEN1. The RI/Ch ratio for *dna2*Δ strain at telomeres is 0.7. At *ARS1*, in contrast, the RI/Ch value for *dna2*Δ drops to 0.02, comparable with WT, which drops to 0.01 (Fig. 6*B*), suggesting efficient conversion of RIs into chromosomal size fragments at ARS1. When the blots were hybridized to a probe recognizing the repetitive ribosomal ARS, the result was the same as that with ARS1, demonstrating that the defect in Fig. 6*B*, *lane 3,* was not due to nonspecific degradation in the sample (data not shown).

These results suggest that Dna2 plays a major role in maturation of RIs at telomeres, even when both FEN1 and Exo1 were present. This is the first demonstration of a locus *in vivo* where Dna2 and the proposed two-nuclease (Dna2 plus FEN1) pathway of lagging strand maturation were functioning.

DISCUSSION

Our studies suggest that Dna2 participates in both telomeric GT-overhang production and CA-strand fill-in (see model in Fig. 7), consistent with the two major known activities of Dna2

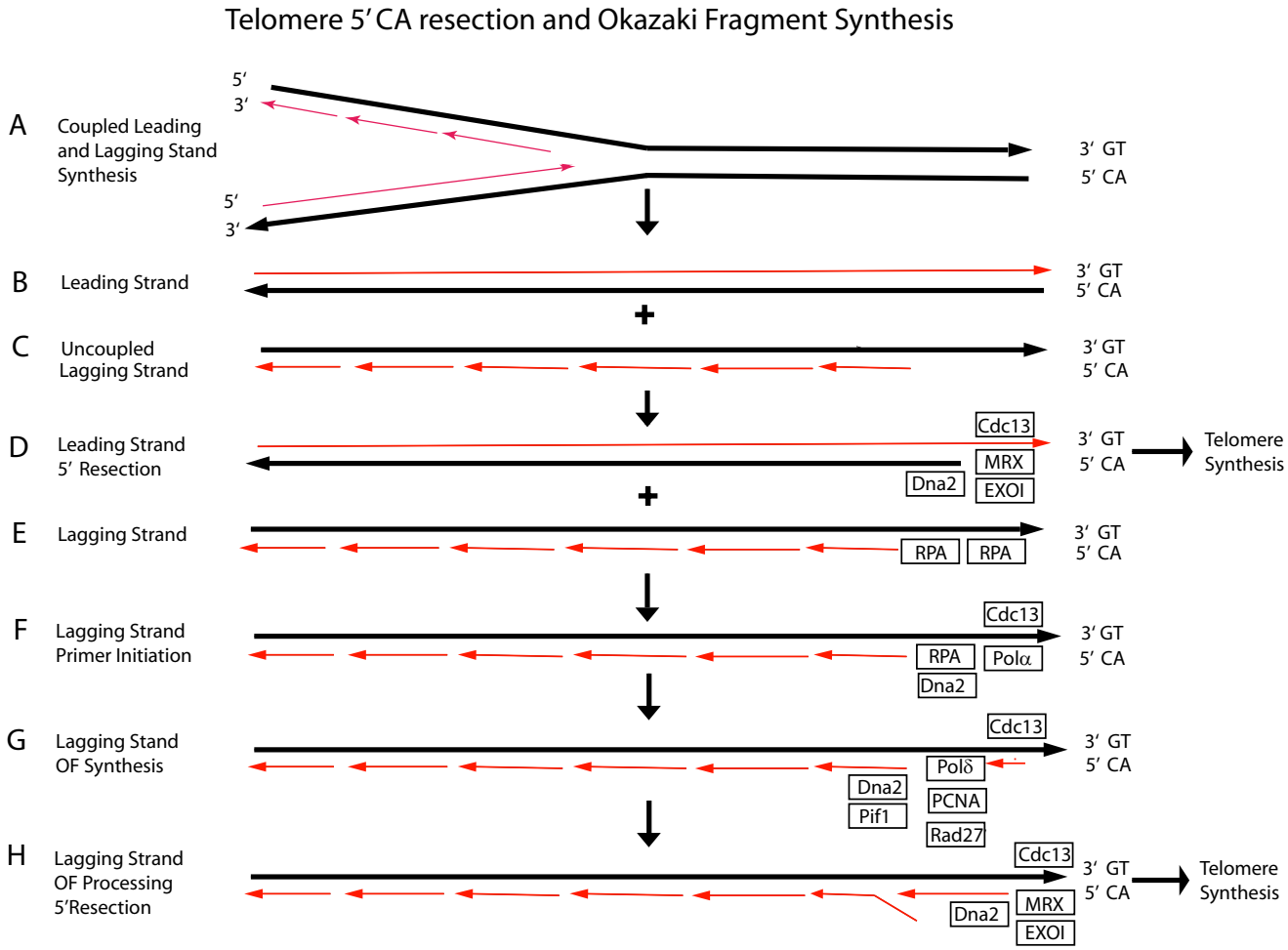

FIGURE 7. **Telomere DNA replication and the proteins involved.** A replication fork is initiated in the subtelomeric region creating forks that replicate templates (*black lines*) outward toward the telomere. The GT-rich strand uses the leading strand polymerase, and the CA-strand uses the lagging strand polymerase. *Left leading strand*, synthesis by the leading strand polymerase results in a chromosome with a blunt end. This end is analogous to the HO endonuclease cut chromosome in the *de novo* telomere assay used in this study. The appearance of the normal 3′-GT-overhang on the leading strand therefore requires 5′- to 3′-nuclease processing. Subsequent binding of Cdc13 would allow telomerase binding and synthesis. Nucleases MRX, Sae2, Dna2, and/or Exo1 may be required for efficient 5′- to 3′-CA resection (21, 58 and this work). *Right lagging strand*, pol δ (lagging strand polymerase) arrives at the telomere significantly later than pol ϵ (leading strand polymerase) (90). After leading strand replication is completed, the helicase presumably falls off, and the leading and lagging strand syntheses are uncoupled. This supports the idea that a 3′-GT-overhang, having at least the size of an Okazaki fragment, appears on the chromosome synthesized by the lagging strand. Further evidence suggesting that a 3′-GT-overhang arises on the lagging strand during its replication is that in an *in vitro* SV40 linear DNA replication assay, leading strand synthesis replicates the DNA to the end but lagging strand synthesis leaves a 500-bp single-stranded gap at the end (102). The appearance of RPA at telomeres coincides with the arrival of pol ϵ suggesting that RPA binds the GT template. In mammalian cells, a special process replaces RPA with telomere-specific DNA-binding proteins that do not activate the checkpoint, and we propose the same occurs in yeast for RPA and Cdc13 (103, 104). These overhangs recruit telomerase, recruit protective telomere capping proteins, such as Cdc13, and themselves can form protective structures such as t-loops (13, 105, 106). 3′-GT tails are the primer for synthesis by telomerase.

indicated by genetic studies (28, 42, 45, 46, 85, 86). Dna2 is known to be required for the two-nuclease, Dna2 plus FEN1, Okazaki fragment processing pathway from genetic and biochemical studies, but this pathway has been proposed to occur only at a subset of sequences *in vivo*, based largely on *in vitro* studies of the coordination of pol δ, proliferating cell nuclear antigen, FEN1, and Pif1 (34–40). Now we provide *in vivo* evidence for the "two-nuclease" model by demonstrating that Dna2 plays a role in RI maturation at telomeres. Thus, even in the presence of FEN1 and Exo1, Dna2 is involved in conversion of RIs to chromosomal length DNA at telomeres. DNA ligase 1, which is required for both the one-nuclease and two-nuclease pathways, is also required for RI joining at telomeres. We were able to detect RIs at the putative lagging strand of the internal early firing origin of replication in the ligase-defective mutant but not in the Dna2 mutants. Although we were surprised to find that single-stranded GT tails accumulate at native telomeres in *dna2 exo1* double mutants, this is also consistent with a role in lagging strand maturation because it is the same phenotype as mutants deficient in DNA polymerase α, which initiates Okazaki fragments, or mutants defective in FEN1 (62, 79, 80, 87). We propose that in the absence of faithful lagging strand synthesis and processing, single-stranded DNA accumulates. The question remaining is why the two-nuclease pathway is required, perhaps preferentially, at telomeres. One possibility is that it has to do with telomeric proteins (Pif1, Cdc13, Rap1, Rif1, and Rif2) influencing replication fork stalling in the repeats, inducing long flaps and a requirement for Dna2. A second possibility is that Dna2, which binds G4-containing DNA more avidly than single-stranded DNA, unwinds G4

DNA, and cleaves G4 DNA, is required to remove inhibitory G4 structures arising either in templates or at stalled forks (43, 54). A more intriguing possibility is that it may be due to the lack of nucleosomes in the repeats, which correlates with the fact (Fig. 6) that the nascent DNA intermediates are longer at telomeres than at ARS1 (this work) or at other internal ARSs (83). Finally, it is possible, as in human cells, that leading and lagging strands become uncoupled before CA-strand fill-in, and therefore fill-in is related to but is not a *bona fide* Okazaki fragment process (8). Our results show that this process nevertheless requires the same machinery involved in Okazaki fragment processing.

We also verified a significant role for Dna2 in telomere resection at *de novo* telomeres. We observed a greater defect in both *de novo* telomere elongation and in resection than did Bonetti *et al.* (58), however, who saw defects only in *dna2 exo1* double mutants. This is most likely explained by the fact that Bonetti *et al.* (58) used conditions semi-permissive for *dna2-1* growth in high salt, whereas our experiments were carried out under fully restrictive conditions. (They needed to do this because *dna2-1 exo1*Δ double mutants are inviable in standard growth media.) High salt and high osmotic media suppress the growth defects of many replication mutants (21), and the mechanism has recently been traced to induction of the stress-activated protein kinase, Hog1, which phosphorylates components of the replication fork such as Mrc1, stabilizing stressed replication forks (78). Interestingly, *dna2-1 hog1*Δ strains are inviable at any temperature (88). Previously, Gottschling and co-workers (21) established that *pol1* mutants that were defective in telomere elongation at the restrictive temperature were competent under semi-permissive temperature conditions, in keeping with the effects being specific for the penetrance of the mutations; in fact, they were even hyperactive. The differences could also be due to the use of different strains, W303 in Bonetti *et al.* (58) and S288C in our work. In addition to differences in strain background, the *de novo* telomere reporter constructs differed, as did the integration of the *dna2-1* mutation. Bonetti *et al.* (58) also failed to detect a resection defect in *dna2*Δ *pif-1m2. pif1* strains themselves affect telomeres. In addition, they are defective in break-induced replication, which may allow increased resection at the *de novo* telomere. Their result may mirror our results with native telomeres in *dna2*Δ *pif1*Δ, *i.e.* very little reduction in overhangs (Figs. 2 and 3), and be due to the fact that Exo1 plays a larger role in *pif1* mutants (58, 89). In any case, we conclude from the reduction and delay that we see that neither Mre11 nor Exo1 can efficiently compensate for the complete absence of Dna2 at a *de novo* telomere under normal growth conditions when nuclear Pif1 helicase is present.

More novel is our finding that resection is different at native telomeres (and on linear plasmids with steady-state telomeres) than it is at internal DSBs or at *de novo* telomeres. Either Dna2 nuclease or Mre11 nuclease is required for resection and repair at a DSB, even in *pif1*Δ (46). At a *de novo* telomere both Mre11 and Dna2 nucleases appear to be required for efficient resection. However, at chromosomal telomeres synthesized during S phase, GT-overhangs, and therefore resection, can occur in the absence of both Dna2 and Mre11 nucleases (at least in a *pif1*Δ strain). The movement of the replication fork through the telomere presumably allows resection in the absence of both Dna2 and Mre11 nucleases. The leading strand polymerase, pol ϵ, may play a critical role in allowing nucleases to process telomere ends, perhaps by uncoupling leading and lagging strands (90). Sgs1 is a partner of Dna2 in DSB resection, and Sae2 is a partner of Mre11 nuclease. *sgs1 sae2*Δ mutants are defective in GT-strand overhang production (58). The difference between *dna2*Δ *mre11-nuclease minus* strains and *sgs1*Δ *sae2*Δ mutants is significant because it must therefore indicate that another nuclease, perhaps Pso2, can carry out resection and that it is modulated by Sgs1 or MRX/Sae2. Pso2 is a 5′-exonuclease related to Apollo, which interacts with MRN and participates in resection of mammalian telomeres (91, 92).

An unanticipated finding was a reproducible G_1 phase population of long 3′-GT tails at both native telomeres and on YLpFAT10-Tel in the *pif1*Δ mutant. Pif1 helicase is an inhibitor of telomerase (93), and the G_1 phase overhangs may be due to excessive telomerase elongation. Pif1 has also been demonstrated to participate in Okazaki fragment processing, however, where it can act as an accessory factor for pol δ, displacing the RNA/DNA primer to produce the long RNA/DNA flaps that require the two-nuclease pathway for RNA/DNA removal (39, 40, 53, 94). Another explanation for the appearance of the telomeric overhangs is, accordingly, incomplete synthesis of the CA-rich strand by pol δ and then further extension of the GT-strands by telomerase in the absence of Pif1. Similarly, the long GT tails could arise as a consequence of enhanced telomere repeat addition in the absence of Pif1 inhibition of telomerase during S phase, leaving the lagging strand polymerases unable to keep up. However, enhanced telomere addition does not necessarily result in greater single-stranded GT tails, because overproduction of Tel1 in a strain with short telomeres stimulates telomere addition and checkpoint activation without an increase in 3′-GT tails (95).

Although the relative contributions of the various nucleases at native telomeres remains to be sorted out, the participation of Dna2 in *de novo* telomere synthesis and resection in *Saccharomyces cerevisiae* appears to be conserved at chromosomal telomeres in *S. pombe.* It is analogous to the requirement for Dna2 for efficient telomere synthesis and CA-strand degradation in *S. pombe* (96). In *S. pombe,* the appearance of 3′-GT tails at telomeres in *taz1*Δ strains is significantly reduced in a *taz1*Δ *dna2-2C* mutant (97). Taz1 is a telomere GT/CA DNA-binding protein, and replication forks stall at telomeres in *taz1*Δ strains (98, 99). This gives rise to a rapid shortening of telomeres that are similarly rapidly repaired by telomerase-catalyzed synthesis of very long telomeres with extensive single strand overhangs (99). These overhangs are generated by resection and fail to appear in *dna2-2C* mutants (97). This result with *taz1*Δ mutants generalizes to telomeres of strains even in the presence of normal Taz1, because the appearance of 3′-GT tails and the binding of telomerase to normal telomeres is also defective in the *dna2-2C* mutant. The *dna2-2C* mutation is in the helicase domain, between helicase motifs II and III (85), but because nuclease and helicase are coupled (100), it may also have compromised nuclease activity. Conservation may extend even further, because mouse embryonic fibroblasts defective in DNA2 exhibit telomere replication defects (43). It will be interesting to

determine to what extent these effects include GT-overhang length and CA-strand fill-in and whether they are conserved in human Dna2 knockdown cells (101).

Acknowledgments—We thank Robert Bambara and Lata Balakrishnan for interesting discussion; David Lydall and Greg Ngo for comments on the manuscript; Piotr Polaczek for preparation of figures; and Dan Gottschling, Charles Boone, and Svetlana Makovets for strains.

REFERENCES

1. Shampay, J., Szostak, J. W., and Blackburn, E. H. (1984) DNA sequences of telomeres retained in yeast. *Nature* **310,** 154–157
2. Walmsley, R. W., Chan, C. S., Tye, B. K., and Petes, T. D. (1984) Unusual DNA sequences associated with the ends of yeast chromosomes. *Nature* **310,** 157–160
3. Larrivée, M., LeBel, C., and Wellinger, R. J. (2004) The generation of proper constitutive G-tails on yeast telomeres is dependent on the MRX complex. *Genes Dev.* **18,** 1391–1396
4. Wellinger, R. J., Wolf, A. J., and Zakian, V. A. (1993) *Saccharomyces* telomeres acquire single-strand TG1–3 tails late in S phase. *Cell* **72,** 51–60
5. Wellinger, R. J., and Zakian, V. A. (2012) Everything you wanted to know about *Saccharomyces cerevisiae* telomeres: beginning to end. *Genetics* **191,** 1073–1105
6. Wellinger, R. J., Ethier, K., Labrecque, P., and Zakian, V. A. (1996) Evidence for a new step in telomere maintenance. *Cell* **85,** 423–433
7. Chai, W., Du, Q., Shay, J. W., and Wright, W. E. (2006) Human telomeres have different overhang sizes at leading *versus* lagging strands. *Mol. Cell* **21,** 427–435
8. Zhao, Y., Sfeir, A. J., Zou, Y., Buseman, C. M., Chow, T. T., Shay, J. W., and Wright, W. E. (2009) Telomere extension occurs at most chromosome ends and is uncoupled from fill-in in human cancer cells. *Cell* **138,** 463–475
9. Faure, V., Coulon, S., Hardy, J., and Géli, V. (2010) Cdc13 and telomerase bind through different mechanisms at the lagging- and leading-strand telomeres. *Mol. Cell* **38,** 842–852
10. Greider, C. W., and Blackburn, E. H. (1985) Identification of a specific telomere terminal transferase activity in *Tetrahymena* extracts. *Cell* **43,** 405–413
11. Kironmai, K. M., and Muniyappa, K. (1997) Alteration of telomeric sequences and senescence caused by mutations in RAD50 of *Saccharomyces cerevisiae*. *Genes Cells* **2,** 443–455
12. Nugent, C. I., Bosco, G., Ross, L. O., Evans, S. K., Salinger, A. P., Moore, J. K., Haber, J. E., and Lundblad, V. (1998) Telomere maintenance is dependent on activities required for end repair of double-strand breaks. *Curr. Biol.* **8,** 657–660
13. Diede, S. J., and Gottschling, D. E. (2001) Exonuclease activity is required for sequence addition and Cdc13p loading at a *de novo* telomere. *Curr. Biol.* **11,** 1336–1340
14. Lundblad, V., and Szostak, J. W. (1989) A mutant with a defect in telomere elongation leads to senescence in yeast. *Cell* **57,** 633–643
15. Lendvay, T. S., Morris, D. K., Sah, J., Balasubramanian, B., and Lundblad, V. (1996) Senescence mutants of *Saccharomyces cerevisiae* with a defect in telomere replication identify three additional EST genes. *Genetics* **144,** 1399–1412
16. Garvik, B., Carson, M., and Hartwell, L. (1995) Single-stranded DNA arising at telomeres in cdc13 mutants may constitute a specific signal for the RAD9 checkpoint (published erratum appears in *Mol. Cell. Biol.* (1996) **16,** 457). *Mol. Cell. Biol.* **15,** 6128–6138
17. Grandin, N., Damon, C., and Charbonneau, M. (2001) Ten1 functions in telomere end protection and length regulation in association with Stn1 and Cdc13. *EMBO J.* **20,** 1173–1183
18. Conrad, M. N., Wright, J. H., Wolf, A. J., and Zakian, V. A. (1990) RAP1 protein interacts with yeast telomeres *in vivo*: overproduction alters telomere structure and decreases chromosome stability. *Cell* **63,** 739–750
19. Hardy, C. F., Sussel, L., and Shore, D. (1992) A RAP1-interacting protein involved in transcriptional silencing and telomere length regulation. *Genes Dev.* **6,** 801–814
20. Gravel, S., Larrivée, M., Labrecque, P., and Wellinger, R. J. (1998) Yeast Ku as a regulator of chromosomal DNA end structure. *Science* **280,** 741–744
21. Diede, S. J., and Gottschling, D. E. (1999) Telomerase-mediated telomere addition *in vivo* requires DNA primase and DNA polymerase α and δ. *Cell* **99,** 723–733
22. Budd, M. E., Tong, A. H., Polaczek, P., Peng, X., Boone, C., and Campbell, J. L. (2005) A network of multitasking proteins at the DNA replication fork preserves genome stability. *PLoS Genet.* **1,** e61
23. Budd, M. E., and Campbell, J. L. (1995) A new yeast gene required for DNA replication encodes a protein with homology to DNA helicases. *Proc. Natl. Acad. Sci. U.S.A.* **92,** 7642–7646
24. Budd, M. E., Choe, W.-C., and Campbell, J. L. (1995) DNA2 encodes a DNA helicase essential for replication of eukaryotic chromosomes. *J. Biol. Chem.* **270,** 26766–26769
25. Budd, M. E., Choe, W.-C., and Campbell, J. L. (2000) The nuclease activity of the yeast Dna2 protein, which is related to the RecB-like nucleases, is essential *in vivo*. *J. Biol. Chem.* **275,** 16518–16529
26. Lee, K.-H., Kim, D. W., Bae, S.-H., Kim, J.-A., Ryu, G.-H., Kwon, Y.-N., Kim, K.-A., Koo, H.-S., and Seo, Y.-S. (2000) The endonuclease activity of the yeast Dna2 enzyme is essential *in vivo*. *Nucleic Acids Res.* **28,** 2873–2881
27. Bae, S.-H., Choi, E., Lee, K. H., Park, J. S., Lee, S. H., and Seo, Y. S. (1998) Dna2 of *Saccharomyces cerevisiae* possesses a single-stranded DNA-specific endonuclease activity that is able to act on double-stranded DNA in the presence of ATP. *J. Biol. Chem.* **273,** 26880–26890
28. Budd, M. E., and Campbell, J. L. (1997) A yeast replicative helicase, Dna2 helicase, interacts with yeast FEN-1 nuclease in carrying out its essential function. *Mol. Cell. Biol.* **17,** 2136–2142
29. Tishkoff, D. X., Boerger, A. L., Bertrand, P., Filosi, N., Gaida, G. M., Kane, M. F., and Kolodner, R. D. (1997) Identification and characterization of *Saccharomyces cerevisiae* EXO1, a gene encoding an exonuclease that interacts with MSH2. *Proc. Natl. Acad. Sci. U.S.A.* **94,** 7487–7492
30. Johnson, R. E., Kovvali, G. K., Prakash, L., and Prakash, S. (1995) Requirement for the yeast *RTH1* 5′ to 3′ exonuclease for the stability of simple repetitive DNA. *Science* **269,** 238–240
31. Chen, C., and Kolodner, R. D. (1999) Gross chromosomal rearrangements in *Saccharomyces cerevisiae* replication and recombination defective mutants. *Nat. Genet.* **23,** 81–85
32. Waga, S., and Stillman, B. (1994) Anatomy of a DNA replication fork revealed by reconstitution of SV40 DNA replication *in vitro*. *Nature* **369,** 207–212
33. Tishkoff, D. X., Filosi, N., Gaida, G. M., and Kolodner, R. D. (1997) A novel mutation avoidance mechanism dependent on *Saccharomyces cerevisiae* RAD27 is distinct from DNA mismatch repair. *Cell* **88,** 253–263
34. Ayyagari, R., Gomes, X. V., Gordenin, D. A., and Burgers, P. M. (2003) Okazaki fragment maturation in yeast. I. Distribution of functions between Fen1 and Dna2. *J. Biol. Chem.* **278,** 1618–1625
35. Bae, S. H., Bae, K.-H., Kim, J. A., and Seo, Y. S. (2001) RPA governs endonuclease switching during processing of Okazaki fragments in eukaryotes. *Nature* **412,** 456–461
36. Rossi, M. L., and Bambara, R. A. (2006) Reconstituted Okazaki fragment processing indicates two pathways of primer removal. *J. Biol. Chem.* **281,** 26051–26061
37. Jin, Y. H., Ayyagari, R., Resnick, M. A., Gordenin, D. A., and Burgers, P. M. (2003) Okazaki fragment maturation in yeast. II. Cooperation between the polymerase and 3′ to 5′ exonuclease activities of pol δ in the creation of a ligatable nick. *J. Biol. Chem.* **278,** 1626–1633
38. Garg, P., Stith, C. M., Sabouri, N., Johansson, E., and Burgers, P. M. (2004) Idling by DNA polymerase δ maintains a ligatable nick during lagging-strand DNA replication. *Genes Dev.* **18,** 2764–2773
39. Pike, J. E., Burgers, P. M., Campbell, J. L., and Bambara, R. A. (2009) Pif1 helicase lengthens some Okazaki fragment flaps necessitating Dna2 nu-

clease/helicase action in the two-nuclease processing pathway. *J. Biol. Chem.* **284,** 25170–25180
40. Rossi, M. L., Pike, J. E., Wang, W., Burgers, P. M., Campbell, J. L., and Bambara, R. A. (2008) Pif1 helicase directs eukaryotic Okazaki fragments toward the two-nuclease cleavage pathway for primer removal. *J. Biol. Chem.* **283,** 27483–27493
41. Balakrishnan, L., and Bambara, R. A. (2013) Okazaki fragment metabolism. *Cold Spring Harb. Perspect. Biol.* **5,** a010173
42. Choe, W., Budd, M., Imamura, O., Hoopes, L., and Campbell, J. L. (2002) Dynamic localization of an Okazaki fragment processing protein suggests a novel role in telomere replication. *Mol. Cell. Biol.* **22,** 4202–4217
43. Lin, W., Sampathi, S., Dai, H., Liu, C., Zhou, M., Hu, J., Huang, Q., Campbell, J., Shin-Ya, K., Zheng, L., Chai, W., and Shen, B. (2013) Mammalian DNA2 helicase/nuclease cleaves G-quadruplex DNA and is required for telomere integrity. *EMBO J.* **32,** 1425–1439
44. Sfeir, A., Kosiyatrakul, S. T., Hockemeyer, D., MacRae, S. L., Karlseder, J., Schildkraut, C. L., and de Lange, T. (2009) Mammalian telomeres resemble fragile sites and require TRF1 for efficient replication. *Cell* **138,** 90–103
45. Zhu, Z., Chung, W.-H., Shi, E. Y., Lee, S. E., and Ira, G. (2008) Sgs1 helicase and two nucleases Dna2 and Exo1 resect DNA double-strand break ends. *Cell* **134,** 981–994
46. Budd, M. E., and Campbell, J. L. (2009) Interplay of Mre11 nuclease with Dna2 plus Sgs1 in Rad51-dependent recombinational repair. *PLoS One* **4,** e4267
47. Cejka, P., Cannavo, E., Polaczek, P., Masuda-Sasa, T., Pokharel, S., Campbell, J. L., and Kowalczykowski, S. C. (2010) DNA end resection by Dna2-Sgs1-RPA and its stimulation by Top3-Rmi1 and Mre11-Rad50-Xrs2. *Nature* **467,** 112–116
48. Shim, E. Y., Chung, W. H., Nicolette, M. L., Zhang, Y., Davis, M., Zhu, Z., Paull, T. T., Ira, G., and Lee, S. E. (2010) *Saccharomyces cerevisiae* Mre11/Rad50/Xrs2 and Ku proteins regulate association of Exo1 and Dna2 with DNA breaks. *EMBO J.* **29,** 3370–3380
49. Kuntz, K., and O'Connell, M. J. (2013) Initiation of DNA damage responses through XPG-related nucleases. *EMBO J.* **32,** 290–302
50. Budd, M. E., and Campbell, J. L. (2000) The pattern of sensitivity of yeast *dna2* mutants to DNA damaging agents suggests a role in DSB and postreplication repair pathways. *Mutat. Res.* **459,** 173–186
51. Zou, L. (2013) Four pillars of the S-phase checkpoint. *Genes Dev.* **27,** 227–233
52. Kumar, S., and Burgers, P. M. (2013) Lagging strand maturation factor Dna2 is a component of the replication checkpoint initiation machinery. *Genes Dev.* **27,** 313–321
53. Budd, M. E., Reis, C. C., Smith, S., Myung, K., and Campbell, J. L. (2006) Evidence suggesting that Pif1 helicase functions in DNA replication with the Dna2 helicase/nuclease and DNA polymerase δ. *Mol. Cell. Biol.* **26,** 2490–2500
54. Masuda-Sasa, T., Polaczek, P., Peng, X. P., Chen, L., and Campbell, J. L. (2008) Processing of G4 DNA by Dna2 helicase/nuclease and RPA provides insights into the mechanism of Dna2/RPA substrate recognition. *J. Biol. Chem.* **283,** 24359–24373
55. Zubko, M. K., Guillard, S., and Lydall, D. (2004) Exo1 and Rad24 differentially regulate generation of ssDNA at telomeres of *Saccharomyces cerevisiae* cdc13-1 mutants. *Genetics* **168,** 103–115
56. Maringele, L., and Lydall, D. (2002) EXO1-dependent single-stranded DNA at telomeres activates subsets of DNA damage and spindle checkpoint pathways in budding yeast yku70Δ mutants. *Genes Dev.* **16,** 1919–1933
57. Bertuch, A. A., and Lundblad, V. (2004) EXO1 contributes to telomere maintenance in both telomerase-proficient and telomerase-deficient *Saccharomyces cerevisiae*. *Genetics* **166,** 1651–1659
58. Bonetti, D., Martina, M., Clerici, M., Lucchini, G., and Longhese, M. P. (2009) Multiple pathways regulate 3′ overhang generation at *S. cerevisiae* telomeres. *Mol. Cell* **35,** 70–81
59. Tsubouchi, H., and Ogawa, H. (2000) Exo1 roles for repair of DNA double-strand breaks and meiotic crossing over in *Saccharomyces cerevisiae*. *Mol. Biol. Cell* **11,** 2221–2233
60. Ivanov, E. L., Sugawara, N., White, C. I., Fabre, F., and Haber, J. E. (1994) Mutants of *XRS2* and *RAD50* delay, but do not prevent, mating-type switching in *Saccharomyces cerevisiae*. *Mol. Cell. Biol.* **14,** 3414–3425
61. Mimitou, E. P., and Symington, L. S. (2008) Sae2, Exo1, and Sgs1 collaborate in DNA double-strand break processing. *Nature* **455,** 770–774
62. Parenteau, J., and Wellinger, R. J. (1999) Accumulation of single-stranded DNA and destabilization of telomeric repeats in yeast mutant strains carrying a deletion of *RAD27*. *Mol. Cell. Biol.* **19,** 4143–4152
63. Bielinsky, A. K., and Gerbi, S. A. (1999) Chromosomal ARS1 has a single leading strand start site. *Mol. Cell* **3,** 477–486
64. Wellinger, R. J., and Zakian, V. A. (1989) Lack of positional requirements for autonomously replicating sequence elements on artificial yeast chromosomes. *Proc. Natl. Acad. Sci. U.S.A.* **86,** 973–977
65. Wellinger, R. J., Wolf, A. J., and Zakian, V. A. (1993) Origin activation and formation of single-strand TG1–3 tails occur sequentially in late S phase on a yeast linear plasmid. *Mol. Cell. Biol.* **13,** 4057–4065
66. Fumagalli, M., Rossiello, F., Clerici, M., Barozzi, S., Cittaro, D., Kaplunov, J. M., Bucci, G., Dobreva, M., Matti, V., Beausejour, C. M., Herbig, U., Longhese, M. P., and d'Adda di Fagagna, F. (2012) Telomeric DNA damage is irreparable and causes persistent DNA-damage-response activation. *Nat. Cell Biol.* **14,** 555
67. Walmsley, R. M., and Petes, T. D. (1985) Genetic control of chromosome length in yeast. *Proc. Natl. Acad. Sci. U.S.A.* **82,** 506–510
68. Ribeyre, C., and Shore, D. (2013) Regulation of telomere addition at DNA double-strand breaks. *Chromosoma* **122,** 159–173
69. Budd, M. E., Antoshechkin, I. A., Reis, C., Wold, B. J., and Campbell, J. L. (2011) Inviability of a DNA2 deletion mutant is due to the DNA damage checkpoint. *Cell Cycle* **10,** 1690–1698
70. Garcia, V., Phelps, S. E., Gray, S., and Neale, M. J. (2011) Bidirectional resection of DNA double-strand breaks by Mre11 and Exo1. *Nature* **479,** 241–244
71. Trujillo, K. M., Yuan, S. S., Lee, E. Y., and Sung, P. (1998) Nuclease activities in a complex of human recombination and DNA repair factors Rad50, Mre11, and p95. *J. Biol. Chem.* **273,** 21447–21450
72. Paull, T. T., and Gellert, M. (1998) The 3′ to 5′ exonuclease activity of Mre11 facilitates repair of DNA double-strand breaks. *Mol. Cell* **1,** 969–979
73. Bressan, D. A., Olivares, H. A., Nelms, B. E., and Petrini, J. H. (1998) Alteration of N-terminal phosphoesterase signature motifs inactivates *Saccharomyces cerevisiae* Mre11. *Genetics* **150,** 591–600
74. Sharples, G. J., and Leach, D. R. (1995) Structural and functional similarities between the SbcCD proteins of *Escherichia coli* and the RAD50 and MRE11 (RAD32) recombination and repair proteins of yeast. *Mol. Microbiol.* **17,** 1215–1217
75. Moreau, S., Ferguson, J. R., and Symington, L. S. (1999) The nuclease activity of Mre11 is required for meiosis but not for mating type switching, end joining, or telomere maintenance. *Mol. Cell. Biol.* **19,** 556–566
76. Zhu, X., and Gustafsson, C. M. (2009) Distinct differences in chromatin structure at subtelomeric X and Y′ elements in budding yeast. *PLoS One* **4,** e6363
77. Formosa, T., and Nittis, T. (1999) Dna2 mutants reveal interactions with DNA polymerase α and Ctf4, a Pol α accessory factor, and show that full DNA2 helicase activity is not essential for growth. *Genetics* **151,** 1459–1470
78. Duch, A., de Nadal, E., and Posas, F. (2012) The p38 and Hog1 SAPKs control cell cycle progression in response to environmental stresses. *FEBS Lett.* **586,** 2925–2931
79. Parenteau, J., and Wellinger, R. J. (2002) Differential processing of leading- and lagging-strand ends at *Saccharomyces cerevisiae* telomeres revealed by the absence of Rad27p nuclease. *Genetics* **162,** 1583–1594
80. Adams Martin, A., Dionne, I., Wellinger, R. J., and Holm, C. (2000) The function of DNA polymerase a at telomeric G tails is important for telomere homeostasis. *Mol. Cell. Biol.* **20,** 786–796
81. Carson, M. J., and Hartwell, L. (1985) CDC17: An essential gene that prevents telomere elongation in yeast. *Cell* **42,** 249–257
82. Makovets, S., Herskowitz, I., and Blackburn, E. H. (2004) Anatomy and dynamics of DNA replication fork movement in yeast telomeric regions. *Mol. Cell. Biol.* **24,** 4019–4031
83. Smith, D. J., and Whitehouse, I. (2012) Intrinsic coupling of lagging-

strand synthesis to chromatin assembly. *Nature* **483,** 434–438
84. Tercero, J. A., and Diffley, J. F. (2001) Regulation of DNA replication fork progression through damaged DNA by the Mec1/Rad53 checkpoint. *Nature* **412,** 553–557
85. Kang, H.-Y., Choi, E., Bae, S.-H., Lee, K.-H., Gim, B.-S., Kim, H.-D., Park, C., MacNeill, S. A., and Seo, Y.-S. (2000) Genetic analyses of *Schizosaccharomyces pombe dna2*$^+$ reveal that Dna2 plays an essential role in Okazaki fragment metabolism. *Genetics* **155,** 1055–1067
86. Cejka, P., and Kowalczykowski, S. C. (2010) The full-length *Saccharomyces cerevisiae* Sgs1 protein is a vigorous DNA helicase that preferentially unwinds holliday junctions. *J. Biol. Chem.* **285,** 8290–8301
87. Adams, A. K., and Holm, C. (1996) Specific DNA replication mutations affect telomere length in *Saccharomyces cerevisiae*. *Mol. Cell. Biol.* **16,** 4614–4620
88. Budd, M. E., Tong, A. H., Polaczek, P., Peng, X., Boone, C., and Campbell, J. L. (2005) A network of multi-tasking proteins at the DNA replication fork preserves genome stability. *PLoS Genet.* **1,** e61
89. Chung, W.-H., Zhu, Z., Papusha, A., Malkova, A., and Ira, G. (2010) Defective resection at DNA double-strand breaks leads to *de novo* telomere formation and enhances gene targeting. *PLoS Genet.* **6,** e1000948-e1000948
90. Moser, B. A., Subramanian, L., Chang, Y. T., Noguchi, C., Noguchi, E., and Nakamura, T. M. (2009) Differential arrival of leading and lagging strand DNA polymerases at fission yeast telomeres. *EMBO J.* **28,** 810–820
91. Bae, J. B., Mukhopadhyay, S. S., Liu, L., Zhang, N., Tan, J., Akhter, S., Liu, X., Shen, X., Li, L., and Legerski, R. J. (2008) Snm1B/Apollo mediates replication fork collapse and S phase checkpoint activation in response to DNA interstrand cross-links. *Oncogene* **27,** 5045–5056
92. Lam, Y. C., Akhter, S., Gu, P., Ye, J., Poulet, A., Giraud-Panis, M. J., Bailey, S. M., Gilson, E., Legerski, R. J., and Chang, S. (2010) SNMIB/Apollo protects leading-strand telomeres against NHEJ-mediated repair. *EMBO J.* **29,** 2230–2241
93. Bochman, M. L., Sabouri, N., and Zakian, V. A. (2010) Unwinding the functions of the Pif1 family helicases. *DNA Repair* **9,** 237–249
94. Stith, C. M., Sterling, J., Resnick, M. A., Gordenin, D. A., and Burgers, P. M. (2008) Flexibility of eukaryotic Okazaki fragment maturation through regulated strand displacement synthesis. *J. Biol. Chem.* **283,** 34129–34140
95. Viscardi, V., Bonetti, D., Cartagena-Lirola, H., Lucchini, G., and Longhese, M. P. (2007) MRX-dependent DNA damage response to short telomeres. *Mol. Biol. Cell* **18,** 3047–3058
96. Ueno, M. (2010) Roles of DNA repair proteins in telomere maintenance. *Biosci. Biotechnol. Biochem.* **74,** 1–6
97. Tomita, K., Kibe, T., Kang, H.-Y., Seo, Y.-S., Uritani, M., Ushimaru, T., and Ueno, M. (2004) Fission yeast Dna2 is required for generation of the telomeric single-strand overhang. *Mol. Cell. Biol.* **24,** 9557–9567
98. Miller, K. M., Rog, O., and Cooper, J. P. (2006) Semi-conservative DNA replication through telomeres requires Taz1. *Nature* **440,** 824–828
99. Cooper, J. P., Nimmo, E. R., Allshire, R. C., and Cech, T. R. (1997) Regulation of telomere length and function by a Myb-domain protein in fission yeast. *Nature* **385,** 744–747
100. Pokharel, S., and Campbell, J. L. (2012) Crosstalk between the nuclease and helicase activities of Dna2: Role of an essential iron-sulfur cluster domain. *Nucleic Acids Res.* **40,** 7821–7830
101. Duxin, J. P., Dao, B., Martinsson, P., Rajala, N., Guittat, L., Campbell, J. L., Spelbrink, J. N., and Stewart, S. A. (2009) Human Dna2 is a nuclear and mitochondrial DNA maintenance protein. *Mol. Cell. Biol.* **29,** 4274–4282
102. Ohki, R., Tsurimoto, T., and Ishikawa, F. (2001) *In vitro* reconstitution of the end replication problem. *Mol. Cell. Biol.* **21,** 5753–5766
103. Gong, Y., and de Lange, T. (2010) A Shld1-controlled POT1a provides support for repression of ATR signaling at telomeres through RPA exclusion. *Mol. Cell* **40,** 377–387
104. Flynn, R. L., Centore, R. C., O'Sullivan, R. J., Rai, R., Tse, A., Songyang, Z., Chang, S., Karlseder, J., and Zou, L. (2011) TERRA and hnRNPA1 orchestrate an RPA-to-POT1 switch on telomeric single-stranded DNA. *Nature* **471,** 532–536
105. Griffith, J. D., Comeau, L., Rosenfield, S., Stansel, R. M., Bianchi, A., Moss, H., and de Lange, T. (1999) Mammalian telomeres end in a large duplex loop. *Cell* **97,** 503–514
106. Nugent, C. I., Hughes, T. R., Lue, N. F., and Lundblad, V. (1996) Cdc13p: A single-strand telomeric DNA-binding protein with a dual role in yeast telomere maintenance. *Science* **274,** 249–252